DYE LASERS

Dye lasers are the most versatile class of lasers. They are based on intense optical excitation of dye molecules, commonly dissolved in organic solvents. The characteristic feature of laser dye molecules that makes them so attractive as laser media is that they exhibit strong absorption and emission (fluorescence) of light over large-wavelength bands. Excitation of dye molecules for laser action is induced by optical radiation from other fixed-wavelength lasers or from flashlamps emitting radiation over large spectral bands. The kinetics of these photophysical processes is such that the fluorescence from excited dye molecules can be converted into a highly directional, coherent laser beam with ultranarrow spectral linewidth that exhibits wavelength variations less than 1 ppm. The wavelength of this highly monochromatic laser beam can be widely tuned over several tens of nanometers. The entire spectrum from near ultraviolet (UV) ($\sim$310 nm) to near infrared (IR) ($\sim$1.3 μm) and up to $\sim$1.7 μm with restricted performance is covered by using different dyes. The high intensity of this fundamental output enables further extension in the vacuum UV (VUV) or IR region using nonlinear optical techniques for frequency conversion. Several references (1,2,19) provide curves showing wavelength ranges covered by different dyes. On the other hand, the broad spectral emission can be exploited for generation of a laser beam consisting of ultrashort optical pulses (10^{-10} s to 10^{-14} s). With such diverse output characteristics, it is not surprising that dye lasers have found extensive use in all areas of basic and applied sciences related to energy, environment, health care, and industry as well as for elucidating fundamental processes in nature. Since its discovery by Sorokin and Lankard in 1966 at IBM, this awesome application potential has ceaselessly engaged the attention of the science and technology community and steadily driven a rapid cooperative growth of new dye laser configurations, molecular engineering of dyes, development of high-power pump sources, and novel applications.

GENERAL CHARACTERISTICS OF DYE LASERS

Lasers based on emission of light from atoms or molecules make use of the discrete quantum energy levels that these particles occupy and transitions between these energy levels, which result in absorption and emission. For laser action, the dye molecules are rapidly excited by absorption of light to a higher energy level such that the population density is more than that in a lower energy level to which the excited mole-

cules may relax by emission of optical radiation. The frequency ν of the radiation emitted is related to the energy difference between the levels, E, by the relation $h\nu = E$. Long before the invention of laser, Einstein had classified the emission transitions between quantum energy levels into two different processes—spontaneous and stimulated emission. In spontaneous emission, the radiation may be emitted in any direction, with arbitrary phase, polarization, and with a frequency distributed within the spectral width determined by the width of the energy levels. In stimulated emission, radiation incident on the excited medium from any source, with a frequency lying within the emission band, forces the excited atoms or molecules to emit radiation at the same frequency, polarization, and direction and with the same phase as that of the incident radiation. With more molecules in the higher energy level (*population inversion*), the rate of stimulated emission exceeds that of absorption, leading to net amplification of the incident radiation. A laser resonator usually consists of curved and/or plane mirrors on opposite sides of the active medium to feed the emitted radiation repeatedly to and fro through the active medium. This serves to enforce amplification of the spontaneously emitted light predominantly along the axis of the resonator, thus helping in the formation of a directed laser output. The divergence of the laser beam is a measure of its directionality and is determined by the transverse field distribution within the cavity. Detailed analysis and experimental evidence show that the transverse field distribution of the laser at any plane inside the resonator exhibits one or more of certain steady-state forms (transverse modes) that repeats itself after every round trip in a specific class of resonators called stable resonators. The stability of the resonators is determined by the curvature of the mirrors, their separation and alignment, and the presence of limiting apertures. The minimum divergence is exhibited by the simplest field distribution (lowest-order transverse mode) that is Gaussian in shape.

The fundamental features that distinguish dye lasers from other lasers is the extent of the width of the energy levels participating in the laser action and the physical processes that lead to such broadening of the levels. These radiative absorption and emission processes involve transitions between well-separated energy levels of some of the electrons in the molecule that are relatively mobile. Dye molecules are large organic compounds having a complex structure with several quantified modes of vibration and rotation. This results in association of a densely spaced distribution of vibrational and rotational energy levels with each electronic state. Therefore, optical transitions take place between the vibrational-rotational levels of different electronic energy states. Perturbation of the vibrational-rotational motion caused by electrostatic interactions and collisions with the molecules of the host medium broadens the energy levels. As a result, dyes exhibit broad absorption bands and an emission band—that is, they are red shifted (vide infra) with respect to the longest-wavelength absorption band (Fig. 1). Amplifier gain exists over a large part of the fluorescence band and allows the wavelength of the dye laser to be tuned over the gain band. The broad absorption band of the dye molecules enables excitation of the same dye by a variety of pump lasers with fixed frequencies, and this adds to the versatility of the dye laser. Intense optical excitation that is possible with such sources, or by intensely driven flashlamps, is necessary to pump dye molecules to the excited state at a rate sufficiently faster than the spontaneous emission rate, in order to create and maintain population inversion.

If both the mirrors forming the resonator cavity have uniform reflectivity over the emission spectrum of the dye, the laser output has a broad spectral width—on the order of several nanometers. To produce a narrowband and tunable output, dispersive optical elements such as gratings and prisms are introduced between the gain medium and one of the end mirrors, often replacing the end mirror itself. When the pump radiation is switched on, initially there is emission of broadband fluorescence from the excited molecules. Gratings and prisms disperse the wavelength contents of this broadband radiation in different directions such that a spectrally narrow band of radiation is fed back, along the resonator axis, to interact with the excited molecules. This effect of highly dispersive elements may be depicted as a high resonator loss at all wavelengths except in a narrow band at the laser wavelength, λ_1 (Fig. 2). As radiation intensity at λ_1 starts growing, the gain or population inversion near λ_1 starts reducing due to higher rate of stimulated emission. Fast thermal interactions between the dye molecules and the solvent ensure that all the excited dye molecules interact with the radiation. In this condition the gain is said to be *homogeneously broadened,* and gain reduction (or *gain saturation*) occurs all over the gain profile. The growth of laser intensity at λ_1 and gain saturation continues until the gain is just sufficient to overcome the loss at λ_1 and a steady-state condition is reached. Thus, homogeneous broadening in dye lasers allows most of the energy available as broadband gain to be extracted within a narrowband laser output. This process of spectral condensation is a key feature that leads to efficient operation of narrowband dye lasers. Even the spectral width of the output of a broadband laser is substantially narrower than the fluorescence width, because emission near the peak of the gain spectral profile grows faster during the repeated transits through the gain medium and saturates the gain.

Tunability of the output wavelength is achieved by changing the orientation of the dispersive element, which changes the center wavelength of the radiation fed back into the cavity. Gratings are more dispersive than prisms. Although somewhat more lossy than prisms, reflective gratings with ruled and specially shaped groove profiles, referred to as

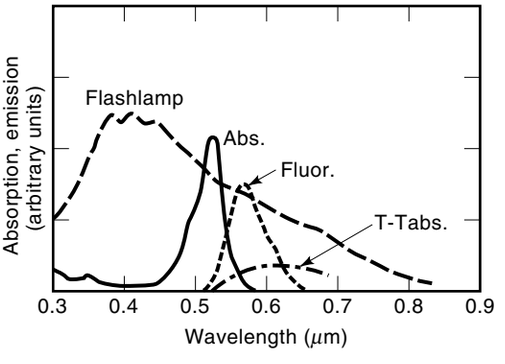

Figure 1. Absorption (solid line) and fluorescence (short dashed line) spectrum of a dye such as Rhodamine 6G in ethanol. Triplet absorption (T-T) often overlaps with fluorescence spectrum. Also shown is a spectrum resembling emission spectrum of flashlamps (dotted line).

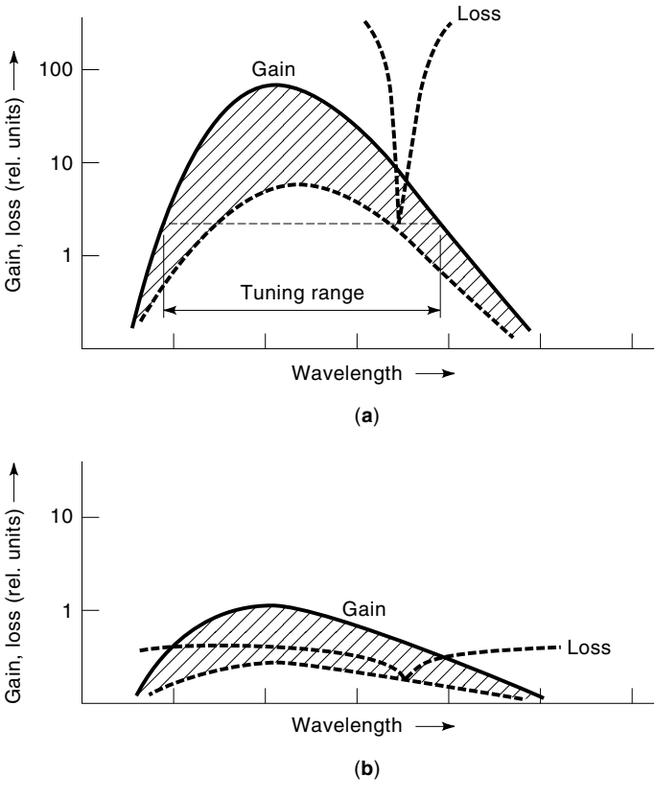

Figure 2. Conceptual comparison of loss management and gain saturation in narrowband short-pulse (a) and CW (b) dye lasers. The high loss (dashed lines) in pulsed dye lasers would not allow laser action in CW laser pumped dye lasers. The low loss in CW dye lasers suffices to restrict lasing to a narrow band due to continued gain saturation, but in pulsed lasers it would allow broadband laser emission to persist for a large fraction of the pulse duration.

blazed gratings, have high efficiency and are commonly used as primary dispersive elements in some classes of dye lasers pumped by pulsed lasers or flashlamps. In these lasers the gain is high enough to tolerate the losses introduced by the gratings.

Interference of electromagnetic waves plays an important role in determining the laser spectrum. Irrespective of the overall bandwidth of the laser, if the spectrum is recorded with high resolution, one observes a comblike pattern of sharp, closely spaced spectral lines, spanning the spectral envelope. This line structure arises because constructive interference occurs at discrete wavelengths at which the intracavity electromagnetic wave at any plane inside the resonator adds exactly in phase with itself after every round trip within the cavity. These cavity resonances or longitudinal modes appear at frequencies $\nu_m = mc/2L(m = \text{integer})$, where L is the optical length of the cavity. Due to constructive interference of multiple waves reflected repeatedly by the end mirrors, the intracavity radiation intensity at these frequencies builds up rapidly. Even slightly away from the resonant frequencies, the waves are superposed with increasing phase lag after every round trip, causing rapid reduction of intensity when a large number of multiply reflected waves participates. Thus, radiation at the resonant frequencies grows at a faster rate and saturates the gain.

Types of Dye Lasers

The diverse family of dye lasers is classified by the nature of the corresponding laser output. *Continuous wave* (CW) dye lasers (1,2) have a continuous, unperturbed output and are usually low-power lasers pumped by CW lasers like argon ion or krypton ion lasers. In comparison to the high-power short-pulse dye lasers, CW dye lasers possess two major advantages. The first is that the minimum output linewidth can be much smaller as it is not limited by the Fourier transform of the output pulse shape. Second, homogeneous broadening of the gain profile of the dye is exploited to the best extent in CW dye lasers. Different wavelength components within the gain spectrum compete for the same overall gain available, and continue to do so, until the wavelength component that sees the maximum net gain (or minimum loss, as determined by the wavelength selective element in the cavity) grows faster and saturates the gain (Fig. 2). Then other wavelength components see a loss more than the saturated gain and are extinguished. With suitable cavity designs it is thus possible to obtain laser oscillation on a single longitudinal mode. The frequency of this cavity mode undergoes small variations due to changes in the optical length of the cavity caused by fluctuations in the gain medium as well as by thermal and mechanical disturbances. Advanced frequency stabilization techniques by servo locking on a stable reference have resulted in commercial lasers with a frequency stability of ~0.002 ppm, whereas laboratory systems with linewidth of better than 1 ppb have been demonstrated. The output linewidth is comparable with that of the narrowest atomic transitions in nature. Thus, CW, single-longitudinal-mode, frequency-controlled dye lasers have found immense applications in opening up a new area of ultra-high-resolution spectroscopy. Some of the major achievements in this area of applications are ultraprecision measurements of the fundamental constants in nature, development of high-precision standards of length and time, ascertaining the validity of quantum theory of particles with increasingly higher precision, cooling and trapping of atoms to ultracold ensembles with temperatures well below a micro-Kelvin, and industrial applications like enrichment of nuclear isotopes for generation of nuclear power.

Flashlamp pumped dye lasers (FLDL) form a different class of lasers with output pulse duration of a few hundred nanoseconds to a few hundred microseconds and have the highest overall efficiencies because the efficiency of flashlamps is much higher than that of lasers (3–5). Xenon-filled flashlamps of linear or coaxial design are generally used for pumping dye lasers. Linear flashlamps have a tubular quartz envelope with tungsten electrodes sealed at the ends. A short-duration high-voltage pulse applied to the electrodes results in intense emission over a large spectral range (Fig. 1). This is coupled to the dye solution by suitably designed enclosures with specular reflectors for imaging the lamp on the dye solution. The dye solution is flown through a cell made of fused silica at a fast speed for removal of heated dye solution between pump pulses. An important design consideration for these dye lasers is to minimize the risetime of the discharge pulses, which is limited by the impedance of the discharge. Preionization produced by a low dc simmer current, or by prepulsing with ~10% of the main pulse, helps in reducing the discharge risetime and also enhances lamp life. Linear flashlamps are used in high-average-power applications. Sys-

tems with 200 W average power at a pulse repetition rate of 50 Hz and an overall efficiency as high as 0.6% have been reported.

For high pulse energy but low repetition rate applications, coaxial flashlamps are used. The dye solution flows through the central tube while gas discharge takes place in the surrounding annular channel. Triaxial and quadraxial tubes are used to provide an intermediate cooling water channel and an evacuated acoustic barrier between the dye tube and the plasma tube. Thermal and shock-wave-induced optical inhomogeneities degrade dye laser beam quality and give rise to wavelength fluctuations. High pulse energies of 400 J have been obtained from coaxial flashlamp pumped dye lasers with an efficiency of 0.8. FLDLs have found limited use in high-resolution spectroscopic applications due to difficulties in eliminating rapid photodegradation of the dye caused by absorption of UV emission from the lamps and because of the short life of strongly driven flashlamps (10^6 to 10^7 pulses).

Pulsed laser pumped dye lasers are capable of providing the best combination of high peak power ($\sim$ several megawatts), repetition rate (10 Hertz to several kilohertz), and minimum linewidth that is limited by the Fourier transform of the pulse (2,4–6). Short-duration (several nanoseconds to a few tens of nanoseconds), pulsed lasers, such as nitrogen lasers, excimer lasers, copper vapor lasers, and fundamental and harmonic outputs of Q-switched solid-state lasers, are used as pump sources. Because of high intensity of the pump lasers, larger resonator losses than for CW lasers can be tolerated, making these lasers much simpler to set up and use. The high pump intensity also permits the use of transverse pumping schemes in which the pump laser is focused by a cylindrical lens onto a dye cell, forming a thin (100 μm to 500 μm) pencil-like (10 mm to 20 mm long) gain region. The depth of the gain region inside the solution is adjusted by changing the dye concentration. The dye laser axis is collinear with the elongated gain region. This design makes the gain length independent of the concentration of the dye and its absorption characteristics at the pump wavelength and allows more flexibility in optimizing the performance of the system.

The large aspect ratio of the gain region also helps in restricting the loss of excitation through amplification of spontaneous emission in directions other than the dye laser axis. Since feedback of narrowband radiation along the laser axis favors its buildup, albeit with a little delay, *amplified spontaneous emission* (ASE) in this direction is suppressed after an initial growth. In a temporal waveform, ASE shows up as a small hump at the beginning of the pulse, especially when the laser is tuned to the ends of the operating wavelength range, where the gain for the narrowband radiation becomes small. However, at very high pump intensities with resultant high gains, ASE in the direction of the gain length may compete better for the gain and increase to the extent where the gain is predominantly saturated by the ASE itself, significantly reducing the efficiency for the narrowband laser output. The presence of ASE in the laser direction degrades the spectral purity of the laser.

Because of inadequate time for spectral narrowing to evolve to its full extent, strongly dispersive elements like gratings are commonly used. Figure 3 shows the two widely used pulse dye laser configurations that are modified versions of those due to Hänsch (7) and Littman and Metcalf/Shoshan et al. (8). In the former, the grating is used in *Littrow* configuration in which it acts as a spectrally selective end mirror. The laser linewidth is determined by the grating dispersion and the divergence of the beam incident on the grating. The divergence is large (few milliradians) because of diffraction of the radiation at the narrow aperture formed by the pencil-like gain region. Current versions employ inclined prisms, instead of an inverted telescope in the old design, to magnify the beam in the plane of grating dispersion. Magnification of a beam reduces its divergence and illuminates a larger number of grating grooves so that the linewidth is reduced. Typical laser linewidths are 0.6 cm^{-1} to 0.2 cm^{-1} ($\Delta\nu/\nu \sim 10^{-4}$ to 10^{-5}) with these systems.

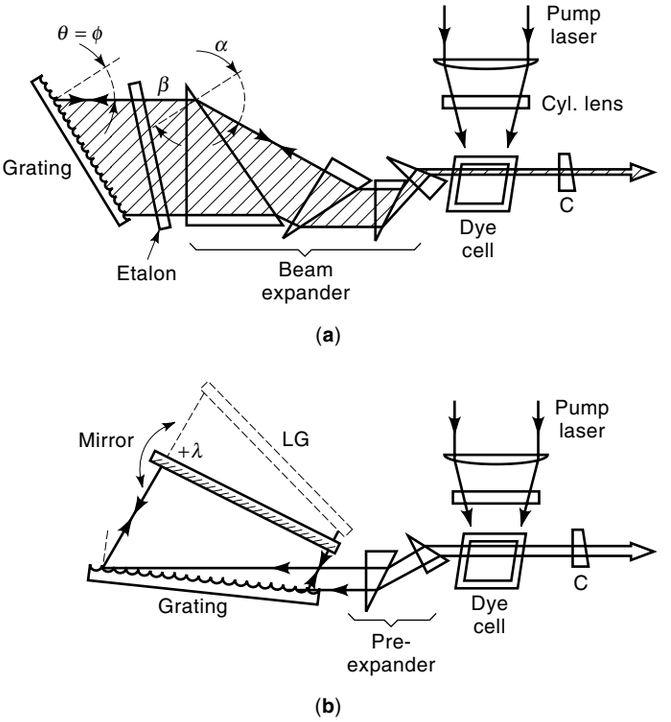

Figure 3. Schematic diagram of a current version of Hänsch (a) and grazing-incidence-grating (b) pulsed dye lasers pumped transversely by short-pulse lasers. C—output coupler, LG—Littrow grating.

For narrower linewidths, Fabry–Perot interferometers are used between the prism beam expander and the grating. A Fabry–Perot interferometers consists of two parallel, highly reflecting mirrors with a constant separation between the mirrors. Either air-spaced or solid interferometers (etalons) made of a single piece of fused silica glass, and coated with dielectric material for reflectivity >85%, are used in pulsed dye lasers. When placed in the path of a collimated beam, they exhibit a series of closely spaced spectrally narrow passbands (Fig. 4) due to interference of multiply reflected light waves passing through. The spectral separation, termed the free spectral range, and the width of the passbands are inversely proportional to the optical path length between the mirrors. Frequency tuning of the passband is easily achieved by tilting the etalon about a suitable axis. Making a judicious choice of the grating and interferometer parameters, it is possible to allow only one passband to be located at the peak of the spectral profile determined by the grating, with the other passbands lying outside the profile. Laser linewidths of

0.03 cm^{-1} (0.9 GHz, $\Delta\nu/\nu \sim 10^{-6}$) in commercial systems and even single longitudinal mode operation ($\Delta\nu \sim 60$ MHz) in laboratory systems have been demonstrated with such resonators (9).

Grazing-incidence-grating (GIG) resonators (Fig. 3) make use of a single grating at a large angle of incidence. An expanded and dispersed beam diffracted by the grating is fed back by a mirror, or by another grating in Littrow configuration, for additional dispersion and narrower linewidth. Tuning is achieved by rotating the mirror or the Littrow grating. Commercial systems with linewidth of 0.05 cm^{-1} are available, and single longitudinal modes of operation have been demonstrated. In comparison to other resonators with same linewidth, GIG resonators are less expensive, easier to align, compact, and offer advantages in terms of continuity of tuning over large-wavelength ranges (which is of particular importance in recording and interpreting spectra). The major drawback of GIG resonators is their lower efficiency due to low diffraction efficiency of the grating at the large angles of incidence at which they are used.

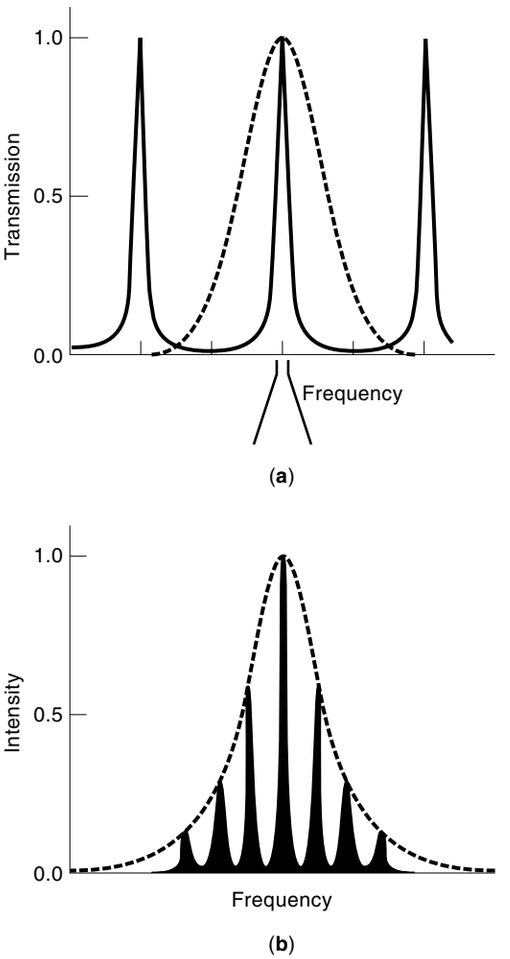

Figure 4. Laser spectrum narrowing with grating and Fabry–Perot interferometer. (a) Solid line shows Fabry-Perot transmission as a function of frequency of transmitted beam. Dashed line shows spectral profile of laser selected by grating alone, allowing only one Fabry–Perot passband. (b) Expanded view of selected passband (dashed line) and longitudinal modes of laser (filled).

Ultrashort pulse dye lasers are broadband lasers in which all the frequency components (longitudinal modes) making up the broad spectrum are forced to oscillate with fixed phase relationships by techniques known as modelocking (10). At a point inside the laser, at some instant of time, all these oscillations arrive in phase and add up to a strong field. Thereafter, the oscillations at different frequencies move out of phase and the resultant field strength reduces. The larger the number of modes, the faster is the reduction in intensity. Since adjacent modes are separated by a frequency difference of $c/2L$, the modes again arrive in step after the cavity round-trip time of $2L/c$. Modelocking ensures that the phase relationships do not change with time. The process is treated mathematically as a Fourier sum of the spectral components. The result is a train of short-duration pulses separated by the cavity round-trip time. Each pulse has a minimum duration limited by the Fourier transform of the laser spectrum. Hence, a large bandwidth as well as a long resonator with a large number of modes (small mode separation) are both desirable. The former enables production of short-duration pulses, and the latter ensures larger separation between pulses with a cleaner baseline. Dye lasers, with broad spectral widths, have played a central role in the development of ultra-short-duration light pulses and investigation of ultrafast processes in nature. Amplification of ultrashort (~100 fs) dye laser pulses in high-energy excimer laser amplifiers, with prior frequency conversion when necessary, has produced few 100 fs pulses with 1 TW (terawatt) to 4 TW output power in the blue UV region (11). Such high-power lasers have opened up a new field of high-intensity laser-matter interaction, with emerging applications in the area of laser-induced fusion technology, compact high-energy electron accelerators, sources of tunable, coherent XUV beams by high-order-harmonic generation, generation of ultrashort X-ray sources, and investigation of fundamental processes in nature.

PHYSICS AND TECHNOLOGY OF DYE LASERS

Photophysical Properties of Dye Molecules

Laser dyes are organic molecules with a large two-dimensional planar structure that is characterized by a chain of conjugated double bonds (alternate single and double bonds), often with benzene-ring-like linkages that tend to rigidize the planar structure (12). Rigidization constrains internal vibration and rotation in the dye molecules, which act as nonradiative (i.e., nonfluorescent) pathways for relaxation of the excited dye molecules. Figure 5 shows the molecular structure of the most commonly used, efficient, and stable laser dye, Rhodamine 6G. Each carbon atom is linked with the neighboring atoms with a single bond or a double bond. One of the two bonds in the double bond (referred to as the π bond) is formed by a transverse overlap of the valence electron orbitals of two carbon atoms such that an electron distribution exists symmetrically above or below the center line joining the two nuclei. The other bond, referred to as the σ bond, is formed by overlap of two other valence orbitals along the axis. In a conjugated molecule, the electrons participating in the formation of the π bond are not attached to any specific pair of carbon atoms but may shift between neighboring pairs. The π electrons are thus relatively mobile. Hence an external elec-

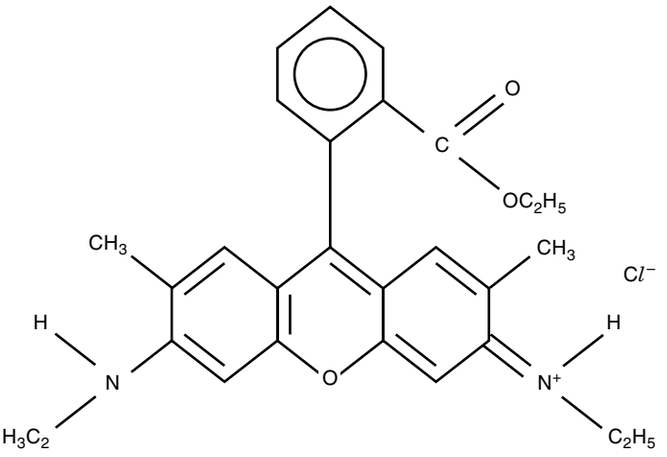

Figure 5. Molecular structure of the most commonly used, efficient, and stable dye, Rhodamine 6G, illustrating the presence of conjugated double bonds.

tromagnetic field of suitable wavelength can easily induce a strong oscillating dipole in the π electron cloud. This results in the strong absorption and emission properties exhibited by dye molecules.

A simple model, called the free-electron model, is often used for elucidating the photophysical properties quantitatively. In this model, the π electrons are assumed to move freely in a one-dimensional box extending over the unfolded length L of the chromophore (the chain of conjugated bonds). Within the box the electrons see an averaged constant potential that rises steeply at the ends of the box. This is a standard exercise in quantum mechanics and predicts that the electrons shall occupy discrete energy levels with energy

$$E_n = n^2h^2/8mL^2 \tag{1}$$

where n is an integer, m is the electron mass, and h is the Planck's constant. In a dye molecule with N number of π electrons the ground electronic state of the molecule is formed by filling up the energy levels up to the $(N/2)$th level, with two electrons having opposite spins in each level. For a stable dye molecule N is an even number as otherwise, even in the ground state, the molecule would have an unpaired electron and would hence be more reactive. The ground state of a laser dye molecule is therefore a singlet state with zero total electronic spin.

A change in the internuclear separation from the equilibrium separation during internal vibration of the molecule leads to an increase in the electronic energy. Figure 6 schematically depicts this dependence in the form of potential energy (PE) curves as a function of the internuclear separation. Vibrational motion is also quantized and depicted as horizontal lines bounded by the PE curve, with the endpoints indicating the location of the turning points. For simple diatomic molecules the coordinate, R, is simply the separation between the nuclei. In a large dye molecule there are several modes of vibration, resulting in multidimensional PE surfaces. The representation in Fig. 6 is therefore schematic in nature, and R may be considered as a generalized vibrational coordinate. The minimum energy for exciting an electron in the dye molecule involves raising an electron from the highest occupied $(N/2)$th level to the lowest unoccupied $((N/2) + 1)$th level. This corresponds to the longest-wavelength absorption band of the dye molecule at a wavelength, λ_m, derived from Eq. (1):

$$\lambda_m = 8mcL^2/h(N+1) \tag{2}$$

In the excited state the two electrons in the $(N/2)$th and $((N/2) + 1)$th level may have parallel or antiparallel spins resulting in the formation of triplet or singlet states, respectively. Figure 6 also shows the PE schematic curves for the excited singlet and triplet states useful for understanding laser action in dyes. In the electronically excited state, S_1, the electron cloud is slightly expanded and exerts less binding force on the nuclei. As a result, the equilibrium separation of the nuclei corresponding to the minimum of the potential well is larger than in the ground state. The triplet states have lower energy than the corresponding excited singlet states. According to the Pauli exclusion principle, no two electrons can have the same spatial, momentum, and spin quantum numbers simultaneously. Hence, on average, wavefunctions of electrons in triplet state with parallel spins have less spatial overlap than those with antiparallel spins in the singlet state. As a result, the Coulomb repulsion component of the electron-electron interaction is less for the electrons in the triplet state, which are, therefore, slightly more bound (lower potential energy).

The vibrational level spacings are $\sim$1200 cm^{-1}, which is much less than the electronic level spacings (>14,000 cm^{-1} in the visible). Rotational motion is also quantized, with level

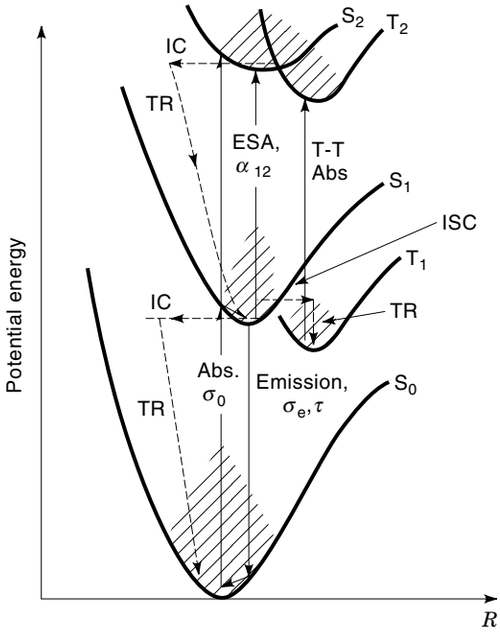

Figure 6. Conceptual depiction of potential energy curves and physical processes influencing laser action. Abbreviations and symbols are explained in text. Cross sections associated with the processes involved in the model discussed are designated by σ with appropriate subscripts. τ denotes the lifetime for spontaneous emission from the first excited singlet state S_0. TR—thermal relaxation.

spacings typically one order of magnitude lower. Perturbation by solvent molecules further broadens these sublevels to form a quasi-continuum that gives rise to the broad absorption and emission spectra due to transition between the sublevels of different electronic states. At room temperature ($kT \sim 200\ cm^{-1}$) there is a Boltzmann distribution of dye molecules in the lowest vibrational-rotational levels of the ground electronic state S_0. Optical transitions between singlet and triplet states have very low probability (referred to as being forbidden transitions in quantum mechanical description) compared to those between singlet-singlet and triplet-triplet states. Depending on the spectrum of the pump radiation source, optical excitation of dye molecules proceeds from the bottom of S_0 to various high-lying sublevels of excited singlet states in accordance with the Franck-Condon principle (i.e., along a vertical line—a result of the fact that, electronic transitions being much faster than nuclear motion, there is no change in nuclear coordinates during an electronic transition). For almost all laser dyes it has been found that nonradiative relaxation from S_2 to S_1 (*internal conversion*) in time scales $\sim$ 10 ps to 0.1 ps, and nonradiative vibrational relaxation (in time scales $\sim$ 1 ps), enhanced by thermal collision with solvent molecules, rapidly brings down the dye molecules to the lowest levels of S_1. Subsequently, the molecules de-excite vertically down to the higher empty sublevels of S_0 by fluorescence emission at slower time scales ($\sim$ few nanoseconds), followed again by rapid nonradiative relaxation down to the bottom of S_0. Note that, due to the shift in the equilibrium separation in S_0 and S_1 the emission band is shifted considerably to longer wavelengths. Due to fast thermal relaxation in comparison to emission rates and small overlap between absorption and fluorescence bands, a population inversion is easily created between the levels taking part in the emission process. Stimulated emission between these levels by a narrowband feedback in the dispersive laser resonator and homogeneous broadening caused by the fast thermal relaxation generate the spectrally condensed narrowband laser output. Fast relaxation (in comparison to excitation rates) to lowest levels of S_1 also allows excitation of all the dye molecules to S_1. This configuration of pumping levels is referred to as a four-level laser scheme, where the population dynamics allow laser action to be achieved at low threshold pump intensity and facilitate CW laser action by recycling the molecules through the different steps.

The parameters that are used to describe the aforementioned processes (Fig. 6) are the transition cross sections (σ), the quantum yield of fluorescence Q_f, and the radiative lifetime τ of the S_1 state. Q_f is defined as the ratio of the number of photons emitted to that absorbed and may be expressed in terms of dye parameters as τ/τ_r, where τ is the total lifetime of S_1 and τ_r is the radiative lifetime. For an efficient laser dye, Q_f should be close to 1. (e.g., 0.93 for Rhodamine 6G). An important nonradiative de-excitation process that reduces Q_f is intersystem crossing (ISC) of dye molecules from singlet to triplet states. Because the triplet to singlet radiative transitions are forbidden, the lowest triplet state is a metastable state that relaxes slowly to the ground state ($\rho_T \sim 10\ \mu s$ to $100\ \mu s$). Thus, ISC removes dye molecules from the lasing cycle, accelerates photochemical degradation of dyes (since molecules with unpaired electrons are more reactive), and, more important, introduces a loss for laser photons by T1 $\rightarrow$ T2 absorption, which may have a substantial overlap with the emission spectrum (Fig. 1). Due to the relatively slow ISC rate ($\sim 3.4 \times 10^6\ s^{-1}$ for Rh6G), ISC starts interfering only for long pulse (flashlamp pumped) or CW dye lasers in which rapid flow of dye solution and presence of triplet quenchers (e.g., oxygen or cyclo-octatetrene dissolved in the solvent) help in reducing the adverse effects.

Other processes that influence laser action are ground-state absorption (GSA from S_0 to S_1) at the laser wavelength, λ_l, and excited-state absorption (ESA from S_1 to S_2) at λ_l and at pump wavelength, λ_p. The strength of GSA at λ_l depends on the tail of the absorption band extending into the emission band. Although weak, the large concentration of dye molecules in the ground state makes its influence significant. GSA is responsible for a red shift of the peak of the gain spectrum from the peak of the fluorescence spectrum. The shift increases with increase in dye concentration and with decrease in pump power. Although a wide variety of pump sources with different wavelengths or with broad spectra may be used for pumping the same dye, use of pump sources with λ_p close to the longest-wavelength absorption band reduces loss of photon energy ($h\nu_p - h\nu_l$) by internal conversion and vibrational relaxation. Nonradiative relaxation of excitation results in heating of the laser active region and generates refractive index gradients and inhomogeneities, which, in turn, leads to distortions in the laser spectrum and beam profile. ESA at either λ_p or λ_l results in a loss for pump or laser photons, which also heats up the medium because of subsequent nonradiative decay to S_1.

Theoretical Model

A rudimentary model of a transversely pumped dye laser consists of a cylindrical region of dye solution of length L with a concentration of N molecules/cc, bounded by two parallel mirrors of reflectivity R_1 and R_2, and pumped uniformly with pump intensity I_p averaged over the absorption depth of the pump radiation in the active medium. The model also assumes that the triplet population is rendered negligible by quenching and removal of dye molecules in the triplet state by flowing. This simplification is more appropriate for short-duration ($\sim$ few tens of nanoseconds) lasers because of the slow rate of ISC. Due to rapid internal conversion, populations in higher excited states are also neglected. Then distributions of molecules in S_0 and S_1 are adequate for describing the process through the population densities N_0 and N_1, such that $N = N_0 + N_1$. The incremental amplification of a light beam of intensity I (photons $cm^{-2} \cdot s^{-1}$) propagating along z direction is expressed as a differential equation:

$$\frac{dI}{dz} = \sigma_e I N_1 - \sigma_0 I N_0 - \sigma_{12} I N_1 \tag{3}$$

where the cross section (as shown in Fig. 6) are taken at the laser wavelength. The different terms describe, in the same sequence, stimulated emission from S_1, GSA from S_0, and ESA from S_1. The population densities are determined by the rate equation

$$\frac{dN_1}{dt} = \sigma_{0p} I_p N_0 - \sigma_e I N_1 + \sigma_0 I N_0 - \frac{N_1}{\tau} \tag{4}$$

Here the last term describes the spontaneous decay of population from S_1. For most practical systems with pulse duration

large compared to τ, the time variations of the laser intensity are slow compared to the spontaneous or stimulated processes and a steady-state approximation is justified. Under this condition, Eq. (3) may be expressed as (13)

$$\frac{1}{I}\frac{dI}{dz} = \frac{g_0}{1+I/I_S} - \frac{SI}{1+I/I_S} \tag{5}$$

Here,

$$g_0 \equiv \frac{\sigma_{\text{eff}} N(\sigma_{0p} I_p \tau - \sigma_0/\sigma_{\text{eff}})}{\sigma_{0p} I_p \tau + 1}$$

with $\sigma_{\text{eff}} \equiv \sigma_e - \sigma_{12}$, is the *small-signal gain coefficient* that describes the single-passage amplification of a weak light beam ($I \ll I_S$) incident along the z direction according to $I(z) = I(0)\exp(g_0 z)$. Moreover,

$$I_S \equiv \frac{\sigma_{0p} I_p \tau + 1}{(\sigma_e + \sigma_0)\tau}$$

is the saturation intensity that determines the extent of gain saturation by the laser, as is clear from the first term in Eq. (5). The increase of I_S with pump intensity represents the fact that at higher pump intensities the molecules brought down to S_0 will be recycled back to S_1 at a *faster* rate; a higher laser intensity is then required to saturate the gain. Finally, the last term in Eq. (5), with

$$S \equiv \frac{\sigma_0 \sigma_{12} \tau N}{\sigma_{0p} I_p \tau + 1}$$

describes a nonlinear loss arising out of absorption of two laser photons by molecules from S_0 and subsequently from S_1 (13). This nonlinear loss due to ESA turns out to be important at shorter wavelengths in the gain spectrum where the absorption from S_0 and hence σ_0 increases.

When the round-trip gain in the cavity is sufficient to compensate for cavity losses arising out of mirror transmissions, absorption, scattering, diffraction at apertures, and losses at other optical elements inside the cavity, laser oscillation sets in and an intense directed laser output is obtained. This threshold gain condition, where small signal gain approximation is not unjustified, is expressed as $R_1 R_2 \exp(2g_0 L) = 1$, with all the losses clubbed into mirror reflectivities. Typical threshold pump intensities predicted by these equations are few tens to hundreds of kW/cm^2 in agreement with experimental results.

The equations just described serve as a starting model for description of the dye laser. Additional equations describing the absorption of pump radiation, especially in longitudinally pumped lasers or amplifiers, evolution of broadband ASE, and triplet state effects, are necessary for more rigorous treatments and are best solved by numerical methods (4). Approximate analytical expressions that are adequate for preliminary analysis of dye oscillators and amplifiers are also available in the literature (2,13–15).

DESIGN CONSIDERATIONS

Pulsed Laser Pumped Narrowband Dye Lasers

Figure 3 shows the two configurations of pulsed narrowband dye lasers commonly used today for linear and nonlinear spectroscopic investigations. The intracavity laser beam at wavelength λ incident on the grating at an angle θ is diffracted at angle ϕ according to the equation

$$a(\sin\theta + \sin\phi) = m\lambda \tag{6}$$

where a is the groove spacing and $m = 0, 1, 2, \ldots$ is the integer order of diffraction. In the Littrow configuration ($\theta = \phi$), commonly used in the Hänsch resonator, one has

$$2a\sin\theta = m\lambda \tag{7}$$

For example, using a grating with 600 grooves/mm at $\theta = 45°$, the Littrow condition will be satisfied for a wavelength of 3.33 m in first-order diffraction, for 1.667 μm in second order, for 666.7 nm in fifth order, and so on. Thus, the same grating may be used for covering the tuning range of all dyes by using the diffraction at different orders. Currently, gratings fabricated by holographic techniques are commonly used because of the absence of ruling errors present in replica gratings made from mechanically ruled master gratings.

In the absence of intracavity beam expanders, the divergence, $\Delta\theta$, of the beam incident on the grating is $\sim\lambda/w$, which is large—typically a few milliradians, mainly due to diffraction at the narrow gain region (diameter $\approx w$). The dispersion of the grating, derived from Eqs. (6) and (7), is given by

$$\frac{d\lambda}{d\theta} = \frac{\lambda}{2\tan\theta} \tag{8}$$

and determines a passive bandwidth for the resonator given by

$$\Delta\lambda_G = \frac{\lambda}{2\tan\theta}\Delta\theta \tag{9}$$

The laser bandwidth is somewhat reduced by gain narrowing and repeated dispersion at the dispersive elements due to a number of round trips in the cavity during the existence of gain. As discussed earlier, the gain narrowing process in these pulsed dye lasers is limited by the short pulse duration.

A prism, used at a large angle of incidence α and at near normal incidence at the exit face (Fig. 3), expands the beam by a factor $M_P \approx \cos\beta/\cos\alpha$, where β is the angle of refraction inside the prism. The divergence of the beam, in the plane of grating diffraction, and hence the passive bandwidth is thereby reduced by the same factor. However, the reflectivity loss at the entrance face of the prism increases rapidly with α as it approaches 90°. Hence, multiple prism beam expanders are used to obtain large magnifications with reduced loss. For identical prisms, the overall loss is minimum when the angles of incidence on all the prisms are same. In commercial narrowband pulsed dye lasers that use such Littrow grating and about 40× four-prism beam expanders, output laser bandwidths of $\sim$0.3 cm^{-1} to 0.6 cm^{-1} (9 GHz to 18 GHz) are available. Duarte (16) provides a detailed discussion on design considerations for prism beam expanders in narrow linewidth dye laser systems.

This linewidth is still too large compared with linewidths of atomic and molecular transitions in vapor samples, especially when such samples are available in the form of collimated beams. In vapor samples, the frequency or wavelength of the directed laser source as seen by the randomly moving atoms

is Doppler shifted to different extents depending on the distribution of velocity components in that direction. The absorption or excitation spectrum is then *Doppler broadened,* with the broadening increasing with vapor temperature and decreasing with the mass of the particles. In high-resolution spectroscopy, Doppler broadening is reduced to a less than a few gigahertz by steering the probing laser in a direction perpendicular to a well-collimated atomic or molecular beam.

As mentioned earlier, to reduce the laser bandwidth further, intracavity Fabry–Perot etalons (FPE) are used. The FPE passbands are centered at wavelengths λ given by

$$2\mu t \cos\theta' = n\lambda \tag{10}$$

where θ' is the angle of refraction inside the etalon and n is the integer-order of the passband. The free spectral range (FSR) of the etalon is given by $(2\mu t)^{-1}$ (in wave numbers, cm^{-1}) or by $\lambda^2/(2\mu t)$ in wavelength units. The sharpness, or the FWHM, of the passband is related to the etalon parameters by $\Delta\lambda_F = FSR/F$, where the finesse, F, is determined (1) by the reflectivity, R, of the coated surfaces, $F_R = \pi\sqrt{R}/(1 - R)$; and (2) by the flatness and parallelism of the surfaces in the illuminated region, $F_F = M/2$, where λ/M is a measure of the deviation from flatness and parallelism across the illuminated region. The overall finesse is given by $F^{-2} = F_R^{-2} + F_F^{-2}$. In practice, using the equations given previously, designers of narrowband dye lasers select grating, beam expander, and etalon parameters such that etalon FSR is slightly larger than the spectral width determined by the grating and beam expander. Other considerations that play important roles in laser design are (1) maximum transmission of etalon, given by $T_m = (1 - R - A)^2/(1 - R)^2$ (where A stands for the fractional absorption and scattering losses introduced by the etalon and its surface coatings), which increases rapidly with reflectivity R and thus reduces the laser efficiency drastically when attempts are made to decrease laser linewidth by increasing the reflectivity finesse; and (2) the divergence, $\Delta\theta$, of the intracavity beam transmitted through the etalon, which contributes to an increase of the etalon passband width, given by $\Delta\lambda_\theta \approx \lambda\theta' \cdot \Delta\theta/\mu^2$, and which increases as the etalon is tilted with respect to the beam for tuning the laser wavelength. Further, as the etalon is tilted, spatial overlap between successive reflected waves from the etalon surfaces decreases and the multiple beam interference process is impeded. This leads to a reduction in finesse and peak transmission. The resultant effect of these factors is to increase laser bandwidth and reduce its efficiency. To minimize these adverse effects, the etalon is placed in the expanded part of the intracavity beam and tilted in the plane of the expanded beam.

Another complication arising out of using an etalon is that, due to the very different dependence of the center wavelengths selected by the grating and etalon on the respective tilt angles, specially designed tilting mechanisms for both are needed such that the center wavelengths are tracked together during wavelength tuning. Degradation of the etalon finesse restricts such synchronized tuning ranges to ~1 nm. After completing one such synchronized scan, the grating is held fixed while the etalon is tilted back to the starting orientation such that a suitable passband is again centered precisely on the wavelength peak currently selected by the grating. Working systems almost invariably employ computerized control for such piecewise continuous wavelength scan using mechanical tilting operations. In some systems, sealed pressure chambers are constructed around the grating and an air-spaced etalon combination with a suitable window for beam entry and exit, to enable synchronized wavelength scanning by changing the pressure of a suitable gas (nitrogen, sulfur hexafluoride, etc.) inside the chamber. Changing the pressure changes the refractive index, μ_{gas}, of the gas and hence the wavelength according to $\lambda_{air} = \mu_{air}\lambda_{gas}/\mu_{gas}$ (6).

The actual laser spectrum, as shown in Fig. 4, consists of the longitudinal modes of the resonator separated in frequency space by $c/2L$ (or $\lambda^2/2L$ in wavelength units), where L is the optical length of the cavity. The frequency of the modes is extremely sensitive to external influences. A change in the cavity length by a small as $\lambda/2$ causes the frequency of a mode to be changed by the separation between the modes themselves. While tuning the wavelength of the laser one actually scans the envelope of the etalon-selected spectral profile over the modes, which may themselves also shift due to change in L during tilting of optical elements. For common applications it is preferable to pack several modes inside the spectral profile by choosing an appropriate cavity length. This is necessary because the intensity of individual modes in such multilongitudinal-mode lasers has been found to fluctuate considerably from pulse to pulse, often with only small subsets of all the longitudinal modes oscillating in individual pulses. Such fluctuations do not show up in time-averaged laser spectra but manifest themselves as randomly fluctuating beat modulations within the temporal profile of successive pulses recorded with a large-bandwidth oscilloscope. When only a few (say, two or three) modes are allowed to oscillate, such fluctuations lead to considerable fluctuations in the output pulse energy. In several applications it is also necessary to maintain a good overlap of the laser spectrum with the absorption spectrum. Fluctuation in mode content of the laser leads to variation in spectral overlap with a narrow atomic transition, or inadequate overlap with an inhomogeneously broadened transition, when the absorption width is similar to, or large compared to, the mode separation, respectively.

A better option, although technologically more complex, is to allow laser oscillations in only a single longitudinal mode by designing a compact cavity with sufficient dispersion so that only one mode lies within the allowed spectral profile. The minimum linewidth of such single-longitudinal-mode dye lasers is dictated by the Fourier transform of the pulse shape. Frequency tuning of these lasers turns out to be technologically more complex than for multilongitudinal-mode narrowbandwidth lasers. The frequency of the mode is tuned by changing the cavity length, with the required submicron precision provided by a piezoelectric transducer that translates a cavity mirror. Simultaneously, the center frequency selected by the intracavity etalon is forced to follow the mode frequency by active servo control. Otherwise, as the etalon-selected profile strays away from the chosen mode and verges on an adjustment mode, mode hopping takes place, with the output frequency switching discontinuously to the latter. Tracking is achieved in very high repetition rate pulsed lasers by introducing a small oscillation in the tilt of the etalon, driven by a piezoelectric actuator (9). The dither in the etalon spectral profile modulates the average output power. The amplitude of modulation increases with frequency detuning between the etalon profile peak and the mode, and its phase

with respect to the drive signal depends on the sign of detuning. Phase-sensitive measurement of the average laser power with the drive signal as a reference provides an error signal that is amplified and fed back to the etalon piezo in the correct phase such that the error signal (and hence detuning) is driven to zero. Although the pressure-scanning technique may be employed as a simpler alternative, frequency control—such as precise tuning to a prespecified frequency or stabilizing the laser frequency by servo control—is very slow in comparison.

The GIG configuration, described earlier, features easy and continuous wavelength tuning by tilting a single element (i.e., the tuning mirror or another grating in Littrow orientation). To achieve laser bandwidths (~1 GHz) comparable to that with Littrow grating etalon configuration, the grating in the GIG resonator is used at large angles of incidence close to 89°, where the grating efficiency is very low (<10%). With the incorporation of prism pre-expanders that allow the use of the grating at smaller angles of incidence, laser efficiency comparable to that of the Hänsch configuration is now possible. Although single-mode operation of GIG resonator and mode-hop free tuning of the output frequency over large ranges (>100 GHz) have been demonstrated in specially designed laboratory systems (17), the need to design a compact cavity precludes the use of prism expanders. As a result, the efficiency of such lasers is limited to about 1%.

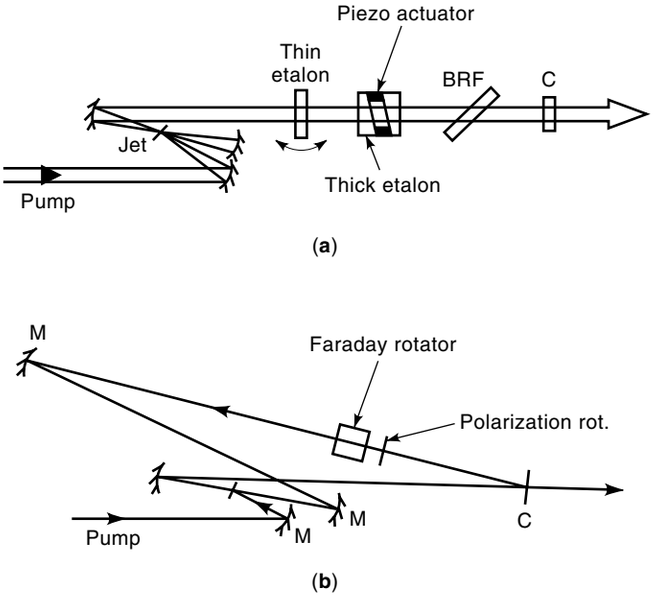

Figure 7. Schematic diagrams of CW dye laser illustrating (a) standing wave resonator with spectral filtering and tuning elements; (b) unidirectional ring resonator (filter and other optical elements for astigmatism compensation and cavity length change are not shown). C—output coupler. M—mirror. BRF—birefringent filter.

CW Narrowband Dye Lasers

Design considerations for CW dye lasers (1,2) differ considerably from those for pulsed dye lasers. Most commonly used CW pump sources are the argon ion and krypton ion lasers, with output powers of 5 W to 25 W distributed over a number of discrete lines in the blue-green (Ar^+ laser) and red (Kr^+ laser) wavelength range. Because of the low output power of CW pump lasers, they are focused tightly (~20 μm to 50 μm diameter) into the dye solution to generate sufficient excitation intensities (~ MW/cm^2) required for pumping CW dye lasers. This tiny excitation region is located within a small, optically flat area of a thin stream (~0.1 mm × 3 mm) of slightly viscous dye solution that is ejected as a free jet from a flat slotted nozzle at velocities of several meters per second. An open tube catches the jet and returns the dye solution to a pump that keeps the dye flowing. The choice of the pump and flow system, consisting of a filter that removes insoluble contaminants, bubbles, and also acts as a buffer to reduce flow fluctuation, is important in narrowband dye laser systems, where fluctuation in the jet thickness or the presence of bubbles lead to wavelength and power fluctuations. Commonly, positive displacement pumps such as gear pumps are used with magnetically coupled drives to prevent contamination of solution and minimize fire hazard arising from leakage of inflammable solvent vapor. The use of free jets, instead of dye cells through which the solution is flown, was motivated by the need to avoid dye cell damage caused by the high focused intensity of the pump laser, especially at the low velocity boundary layers near the cell walls.

Figure 7 shows the schematic of a three-mirror folded resonator in a near-collinear longitudinal pumping geometry used for CW dye lasers. This geometry was a consequence of the need to focus the dye laser radiation at the dye jet for saturating the gain and for maximizing overlap with the gain region. The resonator consists of a short arm in which the dye laser beam is focused and a long arm in which the beam is collimated and coupled out through a flat mirror. Optical elements for spectral narrowing and wavelength tuning are placed in the long arm. The choice of these dispersive elements is dictated mainly by the need to minimize the losses inside the cavity so that reasonable efficiency and large tuning ranges are obtained. For coarse spectral narrowing and wavelength tuning, a birefringent filter (BRF) plate is used. The BRF is oriented at Brewster's angle with respect to the dye laser beam in the long arm of the cavity such that the reflectivity loss of the electric field vector in the plane of incidence vanishes. It consists of crystalline quartz plates with an axis of symmetry, called the optic axis, lying in the plane of the plates and oriented at 45° with respect to the preferred polarization of the electric field vector. Inside the plate, the electric field components of the light wave, polarized along (ordinary) and orthogonal (extraordinary) to the optic axis, travel with different velocities (birefringence) and recombine at the exit face. This results in formation of linearly polarized light in the plane of incidence only for specific wavelengths, at which the phase difference between the ordinary and extraordinary waves is an integral multiple of π. These wavelengths determine the center of the passbands of the BRF at which the losses are minimum. At other wavelengths, components of electric field that are orthogonal to the plane of incidence exist and suffer reflective losses at the surfaces of the BRF. A stack of BRF plates with increasing thickness is used. Only one selected passband of the thinnest BRF lies within the dye gain profile, while the other plates produce progressively narrower passbands (albeit with closer separation) such that a passband of each plate is exactly centered on the main passband. This combination results in the lowest loss in

a narrow wavelength range (FWHM ~ few tens of cm^{-1}) centered on the main passband and higher losses at all other passbands of the thicker plates that lie within the dye gain profile. For wavelength tuning, the BRF stack is rotated in its own plane such that the wavelengths of all the centered passbands track together. Typical laser linewidths of less than 0.1 cm^{-1} containing a large number of longitudinal modes are obtained with the BRF. For restricting the laser oscillation to a single mode, a pair of low-loss and hence low-finesse Fabry-Perot etalons are used. For obtaining the same effective FSR and passband width as that of two etalons in tandem with only one etalon, its surface reflectivities must be increased that would result in higher losses. As a result of unrestricted spectral narrowing, in sharp contrast to pulsed laser pumped dye lasers, less than 1% extra loss for the unwanted modes just away from the peak of the thick-etalon transmission profile is sufficient to restrict lasing in the selected mode located at the peak.

Such survival of the fittest mode is, however, interrupted by the formation of standing wave patterns due to superposition of the counterpropagating light waves in the linear cavity. The standing waves formed by the selected mode at wavelength λ have high intensities at antinodes and low intensities at nodes separated spatially by $\lambda/4$. Consequently, the gain is actually saturated only close to the antinodes in the gain medium—a process aptly referred to as *spatial hole burning*. A second mode in the neighborhood, in spite of a slightly higher loss, may have antinodes at the location of the nodes of the first mode. Spatial hole burning results in unwanted multiple frequency operation, especially at high pump laser powers. In addition, incomplete utilization of the gain by the selected longitudinal mode restricts the laser efficiency in single-mode operation. To overcome the adverse effects of spatial hole burning, current CW dye lasers are also configured as a traveling-wave ring resonator in which a small relative loss (~0.5%) is introduced for one of the two possible counterpropagating waves. This is achieved by using the Faraday effect in a piece of crystal or glass placed in a magnetic field applied parallel to the direction of the propagating light wave. The Faraday effect rotates the plane of polarization of light in a direction independent of the direction of propagation through the material. A polarization rotator (a birefringent crystal plate of appropriate thickness) placed on one side of the material reverses the rotation of the emerging light. The counterpropagating light has its polarization rotated by both the rotator and Faraday effect in the same direction, and therefore suffers higher loss at the several Brewster angle surfaces in the cavity. The small differential loss again suffices for producing unidirectional traveling-wave operation because of continued saturation of gain by the wave in the favored direction. For efficient dyes, unidirectional ring lasers produce almost twice the single-mode output power as that from linear cavity lasers. However, with low gain dyes the increase in threshold due to the insertion loss of the unidirectional device results in lower efficiency than in the linear cavity.

The capability of the CW single-frequency dye laser in ultra-high-resolution spectroscopy is essentially dependent on the monochromaticity (i.e., the time-averaged linewidth and its tunability). The linewidth is determined by fluctuations in the cavity length caused by vibration, fluctuations in the dye jet thickness, ambient air pressure fluctuations, and drifts in the cavity length caused by thermal expansion. With standard procedures like vibration isolation, thermally stable construction and environment, and suitable enclosures, effective time-averaged linewidth of several megahertz is achieved. Various methods of active stabilization techniques have been described in the literature. Most of these make use of the transmission of a small part of the laser output through a highly stabilized, high-finesse (narrow passband) tunable Fabry-Perot interferometer. Transmission at the falling (or rising) edge of the interferometer changes with change in laser frequency and produces the requisite frequency discrimination error signal for feedback control of the cavity length of the laser through a piezoelectric transducer. Commercial stabilized lasers provide effective short-term linewidth of ~1 MHz (about 2 parts in 10^9). The narrowest linewidth of less than 50 Hz (1 part in 10^{13}) has been demonstrated by using sophisticated heterodyne techniques and fast electro-optic modulators that change the cavity length by varying the refractive index of an intracavity crystal by changing an applied electric field.

Tuning the frequency of the laser requires synchronized scanning of the cavity length along with the passbands of the multiple frequency-selective devices. Commercial lasers employ complex electronically controlled drive mechanisms, such as rotating galvo-drives (for the thin etalon and for a near-Brewster plate for cavity length change) and piezoelectric servo-tracking the thick-etalon passband to the scanning cavity mode. This provides a continuous tuning range of ~30 GHz, after which the devices are reset to the initial status, the BRF is stepped to the center of the next 30 GHz range, and the scanning continues. Computer-controlled software and data acquisition can stitch together such piecewise continuous scans to produce an effectively continuous scan over the ~10 THz range.

Pulsed Dye Laser Amplifiers

Several applications of narrowband dye lasers, like investigation of nonlinear optical effects, remote sensing of pollutants in the environment by laser-induced fluorescence, and ultrasensitive detection of trace elements with isotopic selectivity, requires moderate to high laser powers. It is simpler to generate high instantaneous powers in pulsed operation. Amplification of narrowband dye laser oscillator outputs in pulsed laser pumped dye laser amplifiers is a standard technique used for this purpose. Such master-oscillator-power-amplifier (MOPA) concepts resulted from the realization that attempts to obtain high power by pumping narrowband oscillators far above threshold led to an increase of bandwidth and broadband ASE and also generated spurious unwanted spectral components in the laser output. The solution is to constrain the master oscillator operation to produce a low-power, high-quality output that is amplified in one or more dye amplifier stages. The amplifiers usually have a similar transverse pumping configuration that offers design flexibility, but longitudinally pumped amplifiers are also used when beam quality is a prime concern. Frequently, a small fraction (~10%) of the pulsed pump laser is split out, using coated glass plates to pump the oscillator, and the rest is distributed optimally between the following amplifier stages with an optical path delay for synchronization of the oscillator pulse and the pump laser pulse at each stage. The delay is introduced to avoid

amplification of the ASE that exists at the beginning of the oscillator output.

The primary design consideration for pulsed amplifiers is to saturate the gain of the amplifier by a strong signal (oscillator output). Ineffective saturation leads to reduced efficiency and the presence of undesired broadband ASE in the amplifier output coming from single-pass amplification of the spontaneously emitted radiation within the amplifier itself. In other words, the signal should extract the gain in the amplifier efficiently without allowing any spontaneous emission to compete for the gain. High-power dye laser systems are therefore configured in a MOPA chain, such that each amplifier boosts the signal sufficiently to saturate the gain in the following higher-power amplifier. Excessively high signal intensities are, however, detrimental due to increasing nonlinear absorption losses arising from ESA. Integrating Eq. (5) with appropriate initial conditions for an amplifier, one finds that the extraction efficiency of the amplifier exhibits a maximum at an optimum signal intensity (13,14). Extensive recent reviews on capability of high-power dye laser oscillator-amplifier systems may be found in Ref. 18.

Extending the Wavelength Range of Dye Lasers

The short wavelength limit (~310 nm) of dye laser operation arises from photodissociation of dye molecules when the excitation energy due to absorption of UV photons becomes comparable to the bond energy. The long wavelength limit (~1.7 μm) is determined by the short operation life of the molecules because of enhanced chemical reactivity in triplet states to which the molecules are thermally excited, because the triplet states are closer to the ground state for infrared dyes. The fundamental tuning range of abut 310 nm to 900 nm is extended into the VUV and IR regions by nonlinear optical processes, such as frequency doubling and mixing in crystals (19). At the high intensity available with lasers, the oscillating polarization induced in the material shows significant nonlinear dependence on the electric field. If two lasers with electric field components $E_1 \cos \omega_1 t$ and $E_2 \cos \omega_2 t$ and total field $E = E_1 \cos \omega_1 t + E_2 \cos \omega_2 t$ are incident, then the first nonlinear term (proportional to E^2) in a power series expansion of the polarization in terms of the total field contains oscillating components at frequencies $2\omega_1$, $2\omega_2$, and $\omega_1 \pm \omega_2$. These components radiate, respectively, at the second harmonics and the sum or difference frequencies. Since there is no net energy or momentum transfer to the medium, the process becomes significant only when the momentum conservation condition for the photons participating in the process is satisfied. The momentum of a photon propagating in a transparent medium with refractive index μ is given by $\hbar \boldsymbol{k}$, where $\boldsymbol{k}$ is the propagation wave vector of magnitude $k \equiv 2\pi/\lambda \equiv \omega\mu/c$, in the direction of propagation of light. The momentum conservation condition (also referred to as the *phase matching* condition to signify that the two waves propagate with the same phase velocity when they are colinear) for frequency doubling is given by $\boldsymbol{k}(2\omega) = \boldsymbol{k}(\omega) + \boldsymbol{k}(\omega)$. Although, as expressed here, the fundamental photons combining to form one second harmonic photon may, in principle, propagate in different directions, they should be colinear for efficient frequency conversion. The colinear phase matching condition cannot be satisfied in isotropic media due to normal dispersion (monotonic dependence of refractive index on wavelength) at wavelengths away from absorption features in the medium. Fortunately, birefringent crystals such as KDP, KTP, ATP, $LiNbO_3$, and, more recently, β-BaB_2O_4 (BBO) and LiB_3O_5 (LBO), with a high nonlinear response and high damage threshold, have been developed in which efficient frequency conversion is possible. In these crystals, the electromagnetic wave with polarization components parallel (ordinary component) and perpendicular (extraordinary component) to a symmetry axis (*optic axis*) travel with different velocities. In other words, the refractive indices for the two components are different. In addition, while the ordinary refractive index does not depend on the direction of propagation with respect to the optic axis, the extraordinary refractive index does. As a result, it is possible to find a propagation direction in the crystal such that the phase matching condition is satisfied. Tuning of the second harmonic output is achieved by simultaneously tilting the crystal to vary the angle between the incident beam and the optic axis as the fundamental frequency is being tuned. This requires precise angle tilting drives for a few components and is best done under computer or servo control. With frequency doubling and sum frequency mixing, coherent radiation in the wavelength range of about 200 nm to 500 nm has been generated. On the other hand, with difference frequency mixing in $LiNbO_3$ and $AgGaAs_2$, tunable IR radiation over 2.2 μm to 4.2 μm and 4 μm to 9 μm, respectively, has been generated.

Ultrashort Pulse Dye Lasers

Modelocked, ultrashort pulsed dye lasers are essentially broadband CW lasers in which the longitudinal modes are forced to oscillate in phase at precisely defined frequency separation of $c/2L$ between adjacent modes.

In ordinary broadband lasers the longitudinal modes corresponding to the different transverse modes oscillate at different frequencies. Even when forced to operate in the lowest order (Gaussian) transverse mode by placing a small aperture on the axis (which is provided by the gain medium itself), the frequency separation varies slightly from the nominal value of $c/2L$ due to minute pulling of the longitudinal modes toward the center of the gain spectral profile. The relative phases and amplitude of the modes fluctuate in time due to random spontaneous emission within these modes. As a result, the output of broadband CW dye lasers shows transient spikes and fluctuations over a continuous emission level.

Two different techniques for modelocking are commonly employed (10). In passive modelocking, a CW laser is used for pumping the dye laser with a folded, three-mirror, linear resonator configuration similar to that for narrowband CW dye lasers. A saturable absorber dye jet is introduced at a second focus inside the cavity constructed by incorporating two additional curved mirrors. The saturable dye displays increasing transmission with incident intensity due to saturation of the transition (equilization of population in ground and excited states so that there is no net absorption). The modelocking process may be visualized in the spectral domain as follows. When two adjacent modes start growing, the absorber sees an incident radiation with its intensity modulated at the beat frequency. The transmission of the absorber and hence the loss in the resonator is also modulated at the same frequency. Such forced amplitude modulation of the radiation generates sidebands precisely separated by the beat fre-

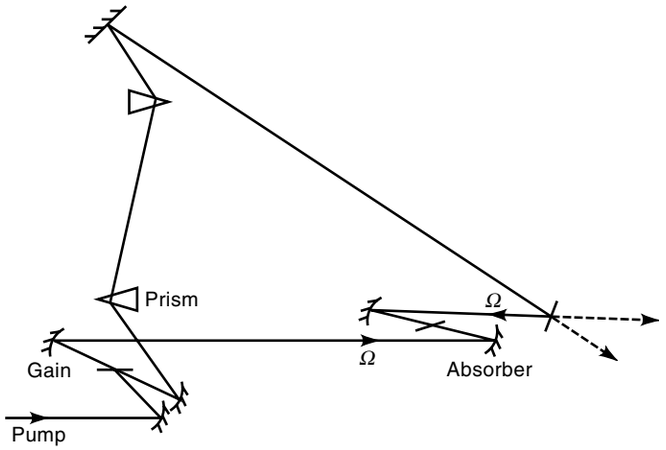

Figure 8. Schematic diagram of a colliding-pulse modelocked (CPM) ultrashort dye laser with intracavity compensation of group-velocity dispersion by prism pairs.

quency and in phase with the driving fields. The coherent sidebands force the evolution of neighboring modes in phase, separated exactly by $c/2L$, and thus initiate modelocking. With increasing numbers of modes evolving in phase, the pulses become sharper and more intense, leading to more effective saturation (and hence lower loss) of the absorber. Irregular low-intensity fluctuations that see a high loss are suppressed. While simple, passively modelocked dye lasers have led to the generation of picosecond pulses, the shortest pulse from a dye laser has been produced in the now famous colliding-pulse modelocked (CPM) ring laser (Fig. 8) (20). In the CPM laser the absorber jet and the gain jet are placed with a separation of one-quarter of the path length around the ring cavity. This is done to ensure that the most favored pulse formation will correspond to counterpropagating (clockwise and anticlockwise) pulses colliding in the absorber jet and arriving at the gain jet with maximum possible time separation (half the round-trip time) such that each pulse of this pair sees the gain recovering to the same value after saturation by the other. These pulses, therefore, have equal amplitudes that result in high-contrast interference when they collide at the absorber jet. This results in more effective saturation by pulses that collide exactly at the absorber. Pulse lengths of ~90 fs have been demonstrated from CPM ring dye lasers.

Further reduction in pulse duration (<30 fs) is obtained by using one or two pairs of prisms inside the cavity, with orientation and separation chosen to compensate for dispersion in the cavity. Material dispersion (dependence of refractive index on wavelength) in the gain jet and the absorber jet leads to variation of group velocity of the pulse with the wavelength that broadens the short pulses. The shortest-duration pulses (~6 fs) were obtained by further compression outside the cavity (21). Pulses with ~50 fs duration were amplified and transmitted through a short length (~ mm) of single-mode silica fiber. Due to nonlinear optical effects at the high intensity in the fiber, the refractive index of the fiber material changes during the pulse. As a result, the velocity of light in the fiber and the phase of the light transmitted are also modulated. The process, referred to as *self-phase modulation,* leads to a time-dependent spectral broadening, or chirping. Subsequently, pairs of gratings and prisms producing an opposite chirp compress the pulse to shorter duration.

Measurement of the duration of such short pulses is done by employing nonlinear optical techniques to determine the spatial overlap of two components of the same pulse as a function of a precisely variable path delay between the two. The nonlinear interaction (such as frequency doubling in crystals) is configured specially so that a signal is detected only when both pulses are overlapping. The resulting autocorrelation trace is deconvoluted, assuming trial pulse shapes, to determine the spatial length of the pulse and hence its duration.

APPLICATION OF DYE LASERS

The majority of applications of dye lasers make use of their diverse properties, such as (1) tunability of the laser, for selective interaction with a particular species; (2) high brightness, for increasing sensitivity and enhancing the response of the application process; (3) focusability, for spatial resolution; and (4) pulse compressibility, for temporal resolution. A few current representative examples are given in this section to illustrate the scope of applications of dye lasers in basic sciences, in industry as diagnostic tools or as process drivers, in environmental monitoring, and in health care. More information may be found in Refs. 19, 22–24.

Laser-Induced Manipulation of Atoms

Dye lasers, and later tunable diode lasers, have been used for cooling and trapping atoms to temperatures less than 20 nK and densities $\sim 10^{11}$/mL (25,26). At these ultra low temperatures the quantum nature of the atomic motion is manifested through the wavelike behavior of atoms, described by the thermal de Broglie wavelength $\lambda_{DB} = \hbar/p$, where p is the momentum of the atom. When the average interparticle separation becomes comparable or less than λ_{DB}, atoms that behave as bosons gather in the lowest-energy quantum state, resulting in *Bose–Einstein condensation* (BEC). BEC is a central feature in understanding the collective behavior of particles, such as superfluidity and superconductivity. Tunable lasers have made it possible, for the first time, to produce and demonstrate BEC in a collection of atoms that are weakly interacting unlike superfluidity in strongly interacting liquid He^4.

The laser technique that led to this fundamental application was recognized by awarding the 1997 Nobel Prize in physics to some of the scientists who had pioneered the field (S. Chu, W. D. Phillips, and C. Cohen-Tannoudji). The basic light-induced process that forces atoms to slow down is the momentum transfer, $(h\nu/c)$, to a moving atom, every time it absorbs a counterpropagating photon from a source tuned to a resonance transition from the ground state. The randomly directed atomic recoil due to spontaneous emission in between successive excitations is canceled out over many absorption-emission cycles because spontaneous emission can be in any direction. For instance, Na atoms moving at average velocity of ~900 m/s from an oven heated to ~600°C would slow down by about 3 cm/s per absorption of a photon (on an average) from a counterpropagating light beam tuned to the 589 nm transition. About 30,000 scatterings would be required to stop the atoms, and the high brightness of the laser helps in achieving this in a short time. To compensate for the chang-

ing Doppler shift of the laser frequency as seen by the decelerating atoms, either the laser frequency is slowly chirped or the atomic transition frequency is tuned by using Zeeman effect in a spatially varying magnetic field. Using such light-induced tunable forces at the intersection of three orthogonal pairs of counterpropagating beams, a slowed-down beam of Na atoms was cooled to a temperature estimated to be ~240 μK. Tunability of the laser again plays a crucial role in the cooling process, for which the laser frequency is tuned slightly below resonance (red detuned). Atoms moving in any direction see counterpropagating light Doppler shifted closer to resonance, whereas the co-propagating light is shifted away from resonance. Thus, the atoms absorb more counterpropagating photons per second, resulting in a frictional force that is proportional to the Doppler shift and hence to the velocity. As a result, in addition to slowing down, the velocity spread is also reduced, and a cold ensemble of atoms remain confined in the viscous *optical molasses* field produced by the laser beams. The atoms, however, cannot be trapped by these momentum transfer forces alone. Lower temperatures and BEC were achieved by innovative cooling techniques and the use of atomic traps constructed with specially shaped magnetic fields and tunable lasers. One compelling signature of BEC was the coherent wavelike motion of the atoms, which manifested itself as an interference pattern between two overlapping condensates released from the trap. Absorption of a laser tuned to the atomic transition was used for observing the pattern.

Laser-cooled and trapped atoms are ideal candidates for precision measurement of frequency because Doppler shift and collision-induced errors are reduced and long measurement times are possible. It is anticipated that the accuracy of the frequency standard, presently based on the Cs atomic clock, may be increased from one part in $\sim 10^9$ to 10^{15}. Manipulation and focusing of atomic beams using tunable lasers have important applications, such as depositing sub-micron-size structures on surfaces—a technique referred to as *atom lithography*. In an electric field E, particles with polarizability α have a potential energy $-\alpha E^2$. For a laser tuned below (red), the transition from the ground state of the atom α is positive. The atom is therefore attracted toward the focus of a nonuniform laser beam by this tunable *optical dipole force.* The standing wave pattern of counterpropagating laser fields blue detuned from the atomic transition forces cooled atoms in an orthogonal beam to collect at the nodes. By placing a silicon substrate close to the standing wave pattern, parallel line structures of ~100 nm width and half-wavelength separation have been deposited (19).

Diagnostic Applications

Several diagnostic applications of dye lasers in science, industry, environmental monitoring, and health care can be found in Refs. 19, 22–24 and other references cited.

Laser-induced fluorescence (LIF) is one of the most widely used ultrasensitive techniques for detection and estimation of atoms, ions, or fluorescent molecules in vapor or condensed phases. Use of pulsed dye lasers offer the advantage of threefold selectivity—selectivity of preferentially exciting a particular species among others; selectivity of the fluorescence spectrum that carries the signature of the species and its concentration; and time-resolved measurement to eliminate interfering fluorescence spectra or Raman scattering from the ambient material. In the microelectronics industry, LIF has been used for monitoring the distribution and temperature of gas phase reactants, in processes such as chemical and physical vapor deposition, plasma etching, and chemical etching during semiconductor processing. Measurement of fluorescence lifetime helps in assessing the sample maturity of crude oil and coal. Time-resolved LIF is being used as a diagnostic tool for ultrasensitive detection and analysis of trace quantities of fluorescent actinides and lanthanides in solution, which are commonly encountered in the nuclear fuel cycle (27). For example, uranium as the uranyl ion (UO_2^{2+}) and other similar ionic forms of Cm, Am, Eu, Tb, Gd, and so on are fluorescent in solutions. Strong and broadband prompt fluorescence from organic chemicals used in spent fuel reprocessing, or present in ground water, severely restricts detection and reliable measurement of these fluorescent species. The delayed fluorescence spectrum suppresses these interferences and makes it possible to detect these elements with ppb (10^{-6} g/L) to ppt (10^{-9} g/L) level sensitivity. The rapidity, selectivity, and sensitivity of these diagnostic techniques are acquiring importance in nuclear waste management for monitoring potential environmental contamination, in monitoring spent fuel reprocessing, and in the health care of uranium mine workers.

Laser-induced photoacoustic spectroscopy (LIPAS) has emerged as another ultrasensitive trace element detection and assay technique, especially when the element is present in weak or nonfluorescent form (19). In LIPAS a pulsed dye laser tuned to an absorption band of the analyte molecule produces a thermal and hence a pressure pulse due to nonradiative (thermal) dissipation of the excitation energy. A pressure transducer, such as a piezoelectric material, is used for detecting the acoustic disturbance as a function of the laser frequency to generate the absorption spectrum. Different valence states of the same element present in different molecular forms in solution exhibit absorption peaks at different wavelengths and are detectable at micromolar to nanomolar concentration levels.

The high intensity at the focus of laser beams gives rise to several nonlinear optical processes, among which coherent anti-Stokes Raman scattering (CARS) has emerged as an important tool for gas phase diagnostics (e.g, in combustion research aimed at improving the thermodynamic efficiency of combustion engines and reducing pollutant emission) (28). Here, two laser beams with frequencies ω_p and ω_s are focused at a common location in the sample, and ω_s is tuned such that the difference $(\omega_p - \omega_s)$ coincides with a Raman active vibrational-rotational mode in a constituent molecule. Since the incident wave frequency coincides with that of the Stokes shifted Raman scattered wave, it creates (together with the pump wave) a coherent excitation of the vibrational-rotational mode of the molecules. In turn, the pump radiation is coherently scattered by the excited molecules to produce a coherent anti-Stokes component at the frequency $\omega_{as} = \omega_p + \omega_p - \omega_s$. Since CARS does not involve any net energy or momentum transfer to the molecule, the efficiency is strongly enhanced only when the momentum conservation condition for the photons is satisfied, as expressed by the phase matching condition, $\boldsymbol{k}_{as} = \boldsymbol{k}_p + \boldsymbol{k}_p - \boldsymbol{k}_s$. The preferred configuration for satisfying the phase matching condition is a converging angular combination of the incident laser beams that results in conve-

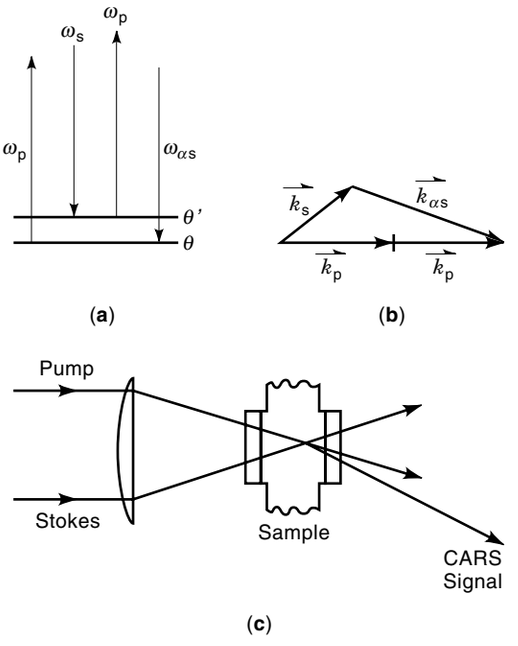

Figure 9. Schematic diagram illustrating CARS. (a) Transitions between molecular energy levels for CARS. (b) Wave vector diagram showing phase matching in non-collinear geometry. (c) Experimental scheme for achieving similar phase matching condition.

nient separation of the CARS beam from the lasers (Fig. 9). The emission of the signal as a separate coherent beam, and the fact that it is at a higher frequency than the incident beams, helps in discriminating against background scatter and LIF at lower frequencies. Measurement of the vibrational-rotational spectra of the constituent molecules and the broadening of spectral lines provides information on species concentration, temperature, and distribution during chemical reactions in the gas phase. CARS has also been applied in determining the temperature and concentration of gases in metallo-organic chemical vapor deposition. Fairly good spectral ($\sim$0.1 cm^{-1}), spatial ($<$1 mm), and temporal ($\sim$ns) resolution is possible with detection limits below 0.1 mbar.

Pulsed dye lasers are being used in environmentally important applications such as remote detection and monitoring of pollutants in the atmosphere and on water bodies. The method, termed LIDAR (light detection and ranging), consists of sending a pulsed laser beam out to the remote target zone and detecting the signal backscattered from absorbing molecules after a time delay that determines the distance of the sampled region. To minimize spreading of the laser beam at a large distance, the beam divergence is reduced by expanding and collimating with a telescope. The same telescope is used for collection of the backscattered signal. Among different variations of LIDAR, differential absorption lidar (DIAL) is a widely used technique that uses two synchronized dye lasers (or other tunable lasers), tuned to the peak and base of an absorption line of the molecule. Some systems use a high pulse repetition frequency dye laser with the facility for rapid wavelength switching between successive pulses. Taking the ratio of the scattered signal at the two wavelengths eliminates unknown contributions to signal attenuation (such as scattering). Measuring the signals with a gated differential delay at times t and $t + \Delta t$ allows determination of absorption due to molecules at a distance of $ct/2$ extended over the path length $c\ \Delta t/2$. Rapid lateral scanning of the laser beam generates a complete air-pollution map at different heights in a short time, and pollution sources are localized for adopting environmental control measures. High-power dye laser oscillator-amplifier systems pumped by the harmonics of Nd : YAG laser, excimer laser, or flashlamp pumped dye lasers are commonly used. Pollutants such as NO_2, SO_2, or NO can be detected with better than ppm level sensitivity at distances up to a few kilometers. Similar techniques have been demonstrated for monitoring the thickness and spreading of oil slicks in oceans. DIAL is also used for monitoring variations in the atmospheric temperature profile with time. Measurement of the broadening of the absorption line of atmospheric sodium, due to thermal-velocity-dependent Doppler shift, by DIAL with narrowband dye lasers provides the temperature information.

Industrial Applications

Since laser radiation is a costly form of energy, the use of dye lasers as industrial process drivers demands high process yields for each photon used and/or high value addition. As an example of the former, Klick (22) has carried out a detailed analysis of photoassisted curing of pigmented polymers using dye lasers instead of UV lamps. Polymers are used as protective coatings in the automobile and appliances industry. The study favors the use of relatively broad-band dye lasers not only for replacement of existing capacity but also for expanding the scope of applications. The polymerization proceeds in a mixture of monomers, oligomers, a photoinitiator (PI), a tertiary amine, and pigment as follows. Absorption of a photon by the PI leads to a proton pick-up from the amine, thus producing a free radical that initiates the polymeric chain reaction. Powdered TIO_2 is used as a white pigment that is nearly opaque. However, the pigment transmission increases with wavelength, whereas the PI absorption decreases, rapidly for both, in the 400 nm to 420 nm region. Since the radiation has to reach the substrate through the coating for uniform curing, the coating efficiency and speed exhibit a maximum at an optimum wavelength. For example, using DETX (2,4-diethylthioxanthone) as PI in a 35 μm thick coating containing 24% by weight of TiO_2 and dye laser pulse energy fluence of 0.05 mJ/cm^2 at 50 Hz repetition rate, the total exposure required for curing showed a minimum ($\sim$24 mJ/cm^2) at a wavelength of 422 nm. The required exposure was doubled for a laser detuned by $\pm$8 nm, which justifies the use of tunable sources. UV lamps or lasers are not suitable for curing pigmented coatings because UV radiation cannot penetrate sufficiently and produces wrinkles due to faster curing at the surface.

Enrichment of uranium in the fissile isotope U^{235} using high-average-power dye lasers is being pursued actively in the United States, Japan, and France (29) for the production of fuel for nuclear reactors. It is projected that the process will be economically more attractive compared to existing technologies based on gas diffusion and high-speed centrifuge and offers scope for better utilization of nuclear fuel resources, because of the high selectivity of the laser-based process. Laser isotope separation (LIS) is an offshoot of the versatile technique called resonance ionization spectroscopy

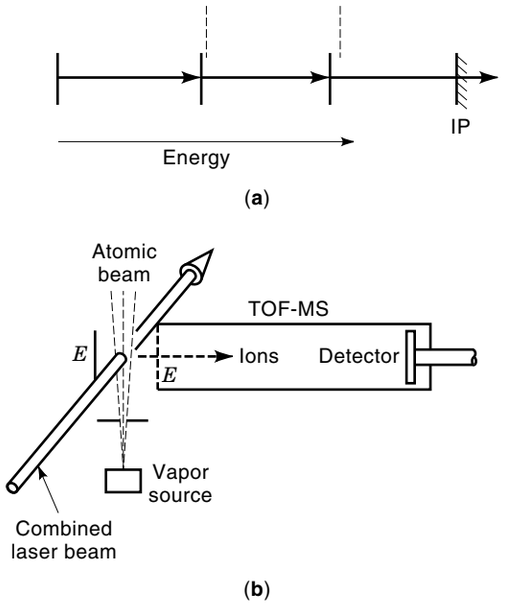

Figure 10. Schematic diagram illustrating multistep resonance ionization process (a) and experimental setup (b). In the diagram shown in (a), three photons of different wavelengths are absorbed successively for ionization of an atom. Alternative schemes are available in Ref. 23. The dashed lines indicate neighboring energy levels of an isotope of the same element or another element that is left unaffected to a large extent. As shown in (b), instead of detection of ions by biased electrodes (E) only, a time-of-flight mass spectrometer (TOF-MS) is often used for identification of isotopes and increasing selectivity. This technique is termed as resonance ionization mass spectrometry (RIMS).

(RIS)—the most sensitive and selective technique for detection and analysis of trace quantities of atoms and isotopes in the vapor phase (23). In practice (see Fig. 10), an atomic beam of the material is produced in a vacuum enclosure by vaporizing the sample and collimating the emerging vapor. The heating is done by electric current, ion beam sputtering, laser melting, and vaporization or by a focused electron beam, depending on the material and the application. Two or more narrowband dye lasers are tuned precisely to transitions of the target isotope or element for excitation from the ground state to successively higher energy levels, resulting in ionization. The ions are collected by biased electrodes placed away from the atomic beam. The combined laser beam is incident at near normal angles on the atomic beam. In this arrangement, the Doppler broadening of the transitions for most elements, including uranium, is small compared to the isotope shift—the small difference in transition frequency between energy levels is due to differences in nuclear mass, size, and charge distribution between the different isotopes. The difference in the transition frequencies of isotopes or of different elements acts as the spectroscopic discriminator that allows narrower-linewidth dye lasers to be used for detection and collection of trace quantities of the target isotope/element with high selectivity in the presence of high concentrations of other isotopes and elements. Multistep sequences enhance selectivity by multiplication of selectivity in each step, provided, of course, that the spectroscopic discrimination in cumulative excitation is not compromised. The efficiency of the process stems from the fact that for pulsed dye laser excitation, atomic transitions can be saturated by relatively small fluence (few μJ/cm^2 to few mJ/cm^2). The pulses from the different dye lasers are synchronized for efficient excitation and ionization. However, high repetition rates on the order of several kilohertz are necessary to avoid loss of atoms flying through a finite-sized interaction zone in between successive laser pulses that would otherwise reduce the sensitivity for trace detection. The high repetition rate ($\sim$4 kHz to 20 kHz) copper vapor laser, its current hybrid variants (which aim to improve the performance by producing low-vapor-pressure copper halides through chemical reactions), and futuristic, high-power diode-laser-array pumped, Q-switched, high-repetition-rate, solid-state lasers are attractive choices as pump lasers for dye lasers used in RIS applications. The dye lasers themselves are technologically more complex, requiring high-speed (several m/s) dye solution flow through specially designed dye cells to remove pump laser-induced thermal gradients between successive pump pulses. In Lawrence Livermore National Laboratory in the United States, one of the most powerful (>2500 W average power), monochromatic ($\Delta\nu/\nu \sim 10^{-8}$), high-repetition-rate (26 kHz) dye laser facilities has been constructed for demonstration of LIS on a plant scale. The facility consists of several chains of copper vapor lasers and dye lasers configured as MOPA systems.

Medical Applications

Dye lasers are finding increasing application in medical treatment and diagnostics. Flashlamp pumped dye lasers are being used for laser lithotripsy—breaking of stones in the ureter or gall bladder by laser radiation. The laser is tuned to the peak absorption wavelength of the stone so as to reduce the power requirement and thus minimize the risk of causing peripheral injuries to the patient. This optimum wavelength depends on the stone composition and is determined by LIF using the same laser at lower power. The laser as well as the LIF signal are carried via an optical fiber that allows less invasive treatment procedures to be adopted.

An important application of dye lasers is in the treatment of cancer by photodynamic therapy (PDT). The patient is injected with a drug, HpD, a derivative of hematoporphyrin ($C_{34}H_{38}O_6N_4$) that is preferentially retained by the malignant tissue. After two to three days the tumor sites are irradiated by laser radiation tuned to the peak of a red absorption band of the drug at $\sim$630 nm, either directly or through an optical fiber, depending on the access to the tumor. Absorption of light initiates a photochemical reaction that destroys the malignant tissue containing HpD and leaves the healthy tissue unaffected. The use of lasers is dictated by the high-energy exposure required ($\sim$ few hundred J/cm^2) and the ease of efficiently coupling the well-directed laser light to an optical fiber.

FUTURE SCOPE

With the arrival of tunable solid-state lasers such as Ti : Sapphire (TiS), semiconductor diode lasers, and the optical parametric oscillator (OPO), replacement of dye lasers in the future is being discussed, debated, and perhaps aggressively projected by commercial manufacturers. The relative merits

of the different systems in the narrowband tunable output regime are discussed here.

Narrowband ($\Delta v < 3$ GHz) TiS lasers pumped by CW argon ion laser or second harmonic of Q-switched pulsed Nd:YAG laser can be tuned over very broad wavelength ranges, about 710 nm to 800 nm in the CW or 680 nm to 980 nm in the pulsed mode of operation. Broadband (~450 GHz) operation over ~670 nm to 1100 nm is possible using different mirrors with optimized reflectivity in different wavelength ranges. High-average-power operation at a high repetition rate is more difficult than in dye lasers due to limitations in power dissipation and nonlinear optical effects. When pumped by pulsed lasers, the long lifetime (~3 μs) of the upper laser level in TiS results in long buildup times (several tens of nanoseconds) for laser action and exhibits large jitter (5 ns to 10 ns). This is not acceptable in applications requiring nanosecond synchronization of different lasers. Extension of the spectral range by frequency doubling leaves a substantial gap in the useful blue-red wavelength region. Additional frequency mixing techniques are employed to cover this range, but at the cost of further reduction in efficiency, increased complexity in synchronized tuning of more optical elements, and requirements for high-power and costly pump lasers to drive all the nonlinear processes efficiently. TiS crystal replacement costs are higher, and tailoring the photophysical properties, as is possible in dye lasers (such as changing dye concentration or solvent), is not feasible. Thus, in spite of comparative drawbacks of dye lasers, such as the use of flowing liquid media that is also toxic and hazardous and hence restrains airborne, submarine, or other field applications, dye lasers will continue to attract users and developers because of their larger wavelength coverage, ease of operation, and lower cost.

Tunable semiconductor diode lasers currently cover wavelength ranges of ~15 nm or more around discrete center wavelengths in the red (635 nm) near IR region (~2 μm). CW single longitudinal mode operation at power levels in the milliwatt range is possible. Emission in the blue–green range has been demonstrated with groups II to VI semiconductors like ZnSe, or by waveguided frequency doubling techniques, but these are in developmental stages. An attractive hybrid configuration would be pulsed amplification of the output of semiconductor diode lasers in pulsed dye amplifiers. Since the diode laser power is too small to saturate the gain in pulsed dye amplifiers, carefully designed regenerative (multipass) amplifiers, or oscillators seeded by the diode laser output, will be necessary to achieve efficient saturation of the amplifier gain and to suppress ASE.

With the development of efficient, high-damage-threshold nonlinear crystals such as β-BaB_2O_4 (BBO) and LiB_3O_5 (LBO), optical-parametric oscillators and amplifiers have emerged as a serious rival to dye lasers due to the unique capability of producing a continuously tunable coherent output over a very wide spectral range [e.g., ~410 nm to 3 μm in BBO pumped by third harmonic of Nd:YAG laser at 355 nm (30)] from a single device. In OPO, when a nonlinear crystal is placed inside a resonator and irradiated with an intense pump laser with frequency ω_p directed along the resonator axis, the nonlinear polarization induced in the crystal generates two outputs, the *signal* and *idler,* at frequencies ω_s and ω_t, respectively, such that $\omega_p = \omega_s + \omega_t$. These new fields grow at the expense of the pump field provided that they are co-propagating and satisfy the phase matching condition, for which the birefringence of the crystal is again exploited. The resonator provides the feedback necessary for efficient generation of a coherent output. For a given orientation of the optic axis of the crystal with respect to the resonator axis, the energy conservation and phase matching conditions together determine the frequencies of the signal and the idler uniquely. Tuning is then simply achieved by tilting the crystal so that the optic axis orientation is changed. In the preceding example, the signal is tunable from 410 nm to 710 nm while the idler, which can be separated from the signal by specially coated beamsplitters, simultaneously tunes from ~3 μm to 710 nm. When pumped three times above threshold, the bandwidth of the signal wave varies from few angströms at 410 nm to several nanometers close to degeneracy at 710 nm ($\omega_s \approx \omega_i$).

For narrowband operation, GIG architecture borrowed from the dye laser configurations has been applied successfully. However, the threshold pump power for OPOs is high in comparison to dye lasers; for the example cited (30), a 12 mm long BBO crystal placed in a ~3 cm long cavity consisting of mirrors of reflectivity >96% and 70% (output coupler) at the signal wavelength range, and transmitting for both idler and pump wavelengths, requires a threshold pump power of 20 MW/cm^2 to 40 MW/cm^2. Focusing a low-power pump laser tightly for generating threshold intensities is counterproductive because in anisotropic birefringent crystals the direction of energy flow (ray direction) is usually different from that of the propagation vector (normal to the wavefront); as a result, the signal wave walks off from the pump wave, faster for a smaller-diameter beam, impeding energy extraction from the pump. For convenient broadband operation above threshold, where optical conversion efficiencies greater than 30% may be obtained, at least 50 mJ/pulse at 355 nm is desirable. In narrowband OPOs the threshold increases substantially due to insertion losses of dispersive elements and increase in cavity length (smaller number of round trips). Further, since the optical parametric process responds almost instantaneously to the changes in the pump laser, multi-longitudinal-mode pump lasers that show strong, intermode beat modulation within the pulse profile are unacceptable for reliable and efficient OPO operation. State-of-the-art pump lasers, injection seeded with single-mode output of diode-array-pumped solid-state laser, are necessary for pumping useful OPOs. The narrower bandwidth of the pump laser in single-mode operation is also important for restricting the available OPO gain within a narrower spectral band that enables better extraction efficiency with narrowband feedback or injection. The pump laser also needs to have exceptionally good beam quality and beam-pointing stability. Due to these several restrictions on the pump laser performance characteristics, the OPO turns out to be a much costlier alternative.

Beam quality, pulse shape, and especially linewidth of pump laser are minor issues in dye lasers. In addition to the high capital cost, chances of damage and costly replacement of OPO crystals or other optics are discouraging aspects that will continue to favor the use of dye lasers for common laboratory-based applications. The requirement of high pulse energy can be relaxed by injection seeding an OPO with a narrowband output from either a dye laser (pulsed or CW) in the signal wavelength range or from tunable diode lasers in the idler range. With the former scheme, a commercial OPO system working at 1 kHz repetition rate with a linewidth of less

than 1 GHz has been marketed, while single-mode operation has been demonstrated in the laboratory with both schemes.

Molecular engineering of laser dyes and improvement of solvent characteristics continue to be challenging areas for improving laser efficiency, arresting photochemical degradation processes, and improving solvent compatibility. An example (31) is the use of *bifluorophoric* laser dyes for increasing efficiency of FLDLs. The optical energy conversion efficiency in FLDLs is limited to <1% because of poor absorption of the wideband flashlamp output by the dye, which exhibits strong absorption over a much narrower band (Fig. 1). To improve the efficiency, energy transfer form the excited singlet state of a shorter wavelength absorber dye (donor) to the laser dye (acceptor) has been investigated extensively. The donor helps in converting a larger part of the flashlamp output into useful excitation of the laser dye. Limited success has been achieved in some cases via radiationless energy transfer of the Foerster type when the fluorescence and absorption band, respectively, of the donor and acceptor overlap. More commonly, singlet to triplet crossing in the donor and subsequent triplet-triplet absorption at the lasing band of the acceptor were found to reduce laser efficiency. A bifluorophoric combination of a donor (*p*-terphenyl) and an acceptor (dimethyl-POPOP) was synthesized in which, due to proximity of the molecules, the energy transfer rates are substantially enhanced compared to singlet to triplet crossing rates in the donor. The engineered molecule showed a reduction in threshold by 10% from that of POPOP alone and by 70% from that of the simple mixture.

As a host medium, water and its isotopic analog, D_2O, possess much better thermo-optical properties than organic solvents, such as large heat capacity and low dependence of refractive index on temperature. Additional advantages are noninflammability, nontoxicity, and ease of disposability. However, due to the high dielectric constant of water, dye molecules aggregate to form nonfluorescing dimers even at the low concentrations required for laser action. Several laser dyes also show poor solubility in water. Both of these drawbacks are alleviated to a large extent by adding detergents such as sodium dodecyl sulfate, cetyl-trimethyl-ammonium bromide, and Triton X-100. Above a certain critical concentration, the detergent molecules or ions are organized into cage-like assemblies or micelles. These micelles incorporate the dye molecules in the interfacial regions or in the surface layers. This helps in solubilization and provides an environment where dimerization is inhibited. In some cases, use of water-surfactant combination has been found to increase fluorescence quantum yield and laser efficiency by rigidizing the dye structure. Jones (32) provides a useful discussion of photochemical tailoring of laser dye properties. Detailed listings of laser dyes are available in Refs. 4 and 33.

Attempts to use dye molecules in the vapor phase with direct discharge excitation have not been successful due to rapid dissociation of molecules. However, laser action in solid-state dye-doped materials is gaining attention due to fabrication of improved hosts, such as modified polymethyl methacrylate (MPMMA), organically modified silicates (ORMOSIL), and other nanocomposites. Narrow linewidth ($\Delta\nu \sim 1.2$ GHz) operation in prism-expander Littrow grating configurations at ~9% efficiency, single-longitudinal-mode operation in GIG resonators, and efficiencies exceeding 60% for broadband emission have been reported. Localized photochemical degradation and slow heat dissipation restrict operation to low repetition rates. Laser output power has been found to reduce by 33% after irradiation with ~20,000 pulses at 0.6 J/cm^2 at a single location. For a discussion and references readers may refer to Ref. 34.

A new approach consists of using two-photon absorption of infrared laser light by new synthesized dyes that leads to excitation of the singlet state, followed by direct upconversion lasing in the visible. Intracavity upconversion lasing in a dye with high two-photon absorption cross section has been demonstrated by placing a dye-solution-filled cell inside the cavity of a Q-switched Nd : YAG laser (35).

It is conceivable that long lengths of MPMMA or ORMOSIL fibers doped suitably with such new dyes and pumped by IR lasers launched into the fiber would act as efficient sources with very low thresholds for frequency upconverted outputs. With feedback provided only at the pump end, the ASE generated at the entrance would travel down the fiber lagging behind the pump pulse and grow in intensity to saturate the gain in the rest of the fiber. Double-ended pumping with suitable delay and pump power distribution may improve efficiency and offer scope for optimization of the device.

BIBLIOGRAPHY

1. L. Hollberg, CW dye lasers, in F. J. Duarte and L. W. Hillman (eds.), *Dye Laser Principles,* New York: Academic Press, 1990.
2. T F. Johnston, Jr., Tunable dye lasers, in *Encyclopedia of Lasers and Optical Technology,* San Diego, CA: Academic Press, 1991.
3. P. N. Everett, Flashlamp-excited dye lasers, in F. J. Duarte (ed.), *High Power Dye Lasers,* Berlin: Springer, 1991.
4. L. G. Nair, Dye lasers, *Prog. Quantum Electron.,* **7**: 153–268, 1982.
5. F. J. Duarte and D. R. Foster, Lasers, dye, technology and engineering, in G. L. Trigg (ed.), *Encyclopedia of Applied Physics,* vol. 8, New York: VCH Publishers, 1994, pp. 331–352.
6. R. Wallenstein, in M. L. Stitch (ed.), *Laser Handbook,* vol. 3, Amsterdam: North-Holland, 1979.
7. T. W. Hänsch, Repetitively pulsed tunable dye lasers for high resolution spectroscopy, *Appl. Opt.,* **11**: 895–898, 1972.
8. (a) M. G. Littman and H. J. Metcalf, Spectrally narrow pulsed dye laser without beam expander, *Appl. Opt.,* **17**: 2224–2227, 1978. (b) I. Shoshan, N. N. Danon, and U. P. Oppenheim, *J. Appl. Phys.,* **48**: 4495, 1977.
9. A. F. Bernhardt and P. Rasmussen, Design criteria and operating characteristics of a single-mode pulsed dye laser, *Appl. Phys.,* **B26**: 141–146, 1981.
10. (a) W. Kaiser (ed.), *Ultrashort Laser Pulsers and Applications,* Berlin: Springer, 1988. (b) P. M. W. French, The generation of ultrashort laser pulses, *Rep. Prog. Phys.,* **58**: 169–267, 1995.
11. (a) S. Watanabe et al., Multiterawatt excimer laser system, *J. Opt. Soc. Am.,* **B6**: 1870, 1989. (b) F. K. Tittel et al., Blue-green dye laser seeded operation of a terawatt excimer laser amplifier, in M. Stuke (ed.), *Dye Lasers: 25 Years,* Berlin: Springer, 1992.
12. F. P. Schäfer (ed.), *Dye Lasers,* 2nd ed., Berlin: Springer, 1990.
13. K. Dasgupta and L. G. Nair, Effect of excited state absorption at signal wavelength in pulsed dye laser amplifiers, *IEEE J. Quantum Electron.,* **QE-26**: 189–192, 1990.
14. K. Dasgupta, S. Kundu, and L. G. Nair, Extraction efficiency of saturated-gain high-power dye laser amplifiers: Effect of nonlinear signal absorption, *Appl. Opt.,* **34**: 1982–1988, 1995.
15. R. S. Hargrove and T. Kan, High-power efficient dye amplifier pumped by copper vapor lasers, *IEEE J. Quantum Electron.,* **QE-16**: 1108–1113, 1980.

16. F. J. Duarte, Narrow linewidth pulsed dye laser oscillators, in F. J. Duarte and L. W. Hillman (eds.), *Dye Laser Principles,* New York: Academic Press, 1990.
17. M. G. Littman, Single-mode pulsed tunable dye laser, *Appl. Opt.,* **23**: 4465–4468, 1984.
18. F. J. Duarte (ed.), *High Power Dye Lasers,* Berlin: Springer, 1991.
19. W. Demtröder, *Laser Spectroscopy,* 2nd ed., Berlin: Springer, 1996.
20. J.-C. Diels, Femtosecond dye lasers, in F. J. Duarte and L. W. Hillman (eds.), *Dye Laser Principles,* New York: Academic Press, 1990.
21. R. L. Fork et al., Compression of pulses to six femtoseconds by using cubic phase compensation, *Opt. Lett.,* **12**: 483–485, 1987.
22. D. Klick, Industrial application of dye lasers, in F. J. Duarte and L. W. Hillman (eds.), *Dye Laser Principles,* New York: Academic Press, 1990.
23. V. S. Letokhov, *Laser Photoionization Spectroscopy,* Orlando, FL: Academic Press, 1987.
24. L. Goldman, pp. 419–432 in Ref. 1.
25. M. H. Anderson et al., Observation of Bose-Einstein condensation in a dilute atomic vapour, *Science,* **269**: 198, 1995.
26. C. S. Adams and E. Riis, Laser cooling and trapping of neutral atoms, *Prog. Quantum Electron.,* **21** (1): 1–79, 1997.
27. C. Moulin et al., Time-resolved laser-induced fluorescence in the nuclear fuel cycle, *Proc. 6th Int. Symp. Adv. Nucl. Energy Res., Innovative Laser Technol. Nucl. Energy,* March 23–25, 1994, Ibaraki, Japan: JAERI, 1995.
28. W. Richter, In situ gas-phase diagnostics by coherent anti-Stokes Raman scattering, in M. Stuke (ed.), *Dye Lasers: 25 Years,* Berlin: Springer, 1992.
29. *Proc. 6th Int. Symp. Adv. Nucl. Energy Res., Innovative Laser Technol. Nucl. Energy,* March 23–25, 1994, Ibaraki, Japan: JAERI, 1995.
30. A. Fix et al., Efficient narrowband optical parametric oscillators of beta-barium-borate (BBO) and lithium-triborate (LBO), in M. Inguscio and R. Wallenstein (eds.), *Solid State Lasers: New Developments and Applications,* New York: Plenum, 1993.
31. F. P. Schäfer, Dye lasers and laser dyes in physical chemistry, in M. Stuke (ed.), *Dye Lasers: 25 Years,* Berlin: Springer, 1992.
32. G. Jones II, Photochemistry of laser dyes, in F. J. Duarte and L. W. Hillman (eds.), *Dye Laser Principles,* New York: Academic Press, 1990.
33. M. Maeda, *Laser Dyes: Properties of Organic Compounds for Dye Lasers,* New York: Academic Press, 1984.
34. F. J. Duarte, Opportunity beckons for solid-state dye lasers, *Laser Focus World,* May 1995.
35. G. S. He et al., Intracavity upconversion lasing within a Q-switched Nd : YAG laser, *Opt. Commun.,* **133**: 175–179, 1997.

KAMALESH DASGUPTA
Bhabha Atomic Research Center

DYNAMICAL SYSTEMS. See LINEAR DYNAMICAL SYSTEMS, APPROXIMATION.

DYNAMIC DATA STRUCTURES. See LIST PROCESSING.